SCHOOL OF ELECTRICAL, ELECTRONICS AND COMPUTER ENGINEERING

SMART INDUCTION COOKING SYSTEM USING SOLAR ENERGY

By

Bandile Innocent Sibiya

211537771

In Partial Fulfilment of the Master of Science in Engineering, College of Agriculture, Engineering and Science, University of KwaZulu-Natal

01 December, 2017

Durban, Glenwood

Dr Chitra Venugopal

EXAMINER’S COPY

UNIVERSITY OF KWAZULU-NATAL

CERTIFICATE

As the candidate's Supervisor, I agree to the submission of this thesis.

…………………………………

(Supervisor: Dr. Chitra Venugopal)

DECLARATION 1 – PLAGIARISM

I, Bandile Innocent Sibiya declare that;

1. The research reported in this thesis, except where otherwise indicated is my original research.
2. This thesis has not been submitted for any degree or examination at any other university.
3. This thesis does not contain other persons' data, pictures, graphs or other information, unless specifically acknowledged as being sourced from other persons.
4. This thesis does not contain other persons' writing, unless specifically acknowledged as being sourced from other researchers. Where other written sources have been quoted, then:
    - Their words have been re-written but the general information attributed to them has been referenced
    - Where their exact words have been used, then their writing has been placed in italics and inside quotation marks, and referenced.
5. This thesis does not contain text, graphics or tables copied and pasted from the Internet, unless specifically acknowledged, and the source being detailed in the thesis and in the References sections.

Signed:

……………………………………

(Bandile Innocent Sibiya)

DECLARATION 2 – PUBLICATIONS

Publication 1

This research has been presented in the First International Conference on Power Engineering, Computing and CONtrol, PECCON-2017 and published in Science Direct

Bandile, I. Sibiya and Dr.Chitra Venugopal, “Solar Power Induction Cooking System”, Energy Procedia, Elsevier, 117(2017), pp.145-156.

Signed:

……………………………………

(Bandile Innocent Sibiya)

ACKNOWLEDGEMENTS

I am greatly indebted to my supervisor Dr Chitra Venugopal for giving me right ways of approaching the research study, good guidance, encouragement at all time and checking of progress now and then to keep me up to date.

I am also greatly indebted to Mr Wikus Coetzee from Microcare, for his advises in terms of solar renewables as he is a specialist and a manufacture.

I would like to thank Mr Renay, Engineering Masters student on campus for helping me on the programming part of the study.

I would also like to appreciate the support received my mom and the rest of the family by encouraging me all the way since started my research in 2016.

I would like to thank my friend Nkosingiphile Mbele who was also doing his research in Criminology for encouraging each other towards completing our thesis this year.

I would to thank specifically my brother Mthobisi Sibiya for keeping me awake while I have to complete the compile of my thesis.

UNIVERSITY OF KWAZULU-NATAL

Abstract

Solar energy presents a good, clean and a reliable source of energy for the future. The focus includes the department of energy strategy (DoE) to allow solar renewables appliances to grow and contribute to the country's economy and global environment. This study uses the recent advantage of induction cooking methods in the market to apply more efficient and economical techniques that go in line with the future wishes in the energy sector. Induction cooker is proven to transfer at least 80 % of the power generated to the pot, while electric stove and gas burners generate more to compensate for the power that is transferred to the atmosphere in the form of heat (i.e. about 55 % efficient). The induction cooker is currently presenting best cooking technology thus far. Though all including induction cooker are completely dependent on the grid power. The research comes with the idea of solar energy to fill the big existing gap of completely depending on non-renewable resources. The advantage comes with the idea of making the product a completely standalone, reducing electricity bills, simple and reliable, no fuel costs and spills, flexible in power sources, sustainable development etc. The proposed cooking technology is improved version and it gives more in the customer needs with regard to clean system, ease to use, conservation and price. Though initial system installation price is high but after five years, the user will be saving a large amount of money. The research will improve the annual savings by 45 % as per the DoE analysis in the comparison of cooking technologies. The thesis focuses on the solar as a primary source of energy to promote savings. The grid power is still used as a backup power source as we are not yet 100 % green but gradually adjusting. The design uses the power auto switching method to treat solar power as a primary source of supply and mains to be the system backup. The cooker battery storage is charged by the solar using efficient MPPT technology and supply the stove at the same time. The mains only take over when the solar is completely not available for some time and it will supply the cooker directly via AC to DC power supply unit and also charges the battery storage via AC to DC battery charger. All the above switching is programmed and happens automatically via remote programmable relay. System design includes theoretical background in the form of circuit analysis, power flow and mathematical calculations. The simulation and practical results present eight different power levels that are displayed in the liquid crystal display (LCD) in the form of switching frequency and power consumed by the load. The power mathematical calculations, Simulations and practical results analysis show a similar trend. The pot material is kept constant while changing switching frequency to achieve desired outputs. Theoretical and simulations are in line while practical differ slightly due to many factors like component internal resistances, conductors used and component internal circuit topology. The other adjustments in practical includes a smaller scale of power (600 watts maximum) compared to simulations due to safety reasons on my capacity to implement a prototype and proving the working of the study at a smaller scale which can be extended if required. The general and specific objectives of the study are achieved in simulations and practical though some adjustments were made during practical in order to me general and specific objectives. The study proves the theory of energy savings, being standalone product in the practical results analysis and thus presents many advantages in the commercial sector for the future.

Table of contents

Table of figures

Table of tables

Abbreviations

DoE	Department of Energy
AC	Alternating Current
DC	Direct Current
LCD	Liquid Crystal Display
MPPT	Maximum Power Point Tracking
CO_2	Carbon Dioxide
PWM	Pulse Width Modulation
V	Volts
A	Amperes
AH	Amperes-Hour
IGBT	Insulated Gate Bipolar Transistor
PV	Photovoltaic
W	Watts
$V_{s.}$	Voltage Source
$C_{r.}$	Resonant Capacitor
ZVS	Zero Voltage Switching
SW	Square Wave
Rs.	Rupee
FEM	Finite Element Model
CB	Circuit Breaker
V_L	load Voltage
RCL	Resistor-Inductor-Capacitor
ZCS	Zero Current Switching
KHz	Kilohertz
RMS	Root Mean Square

1 Introduction

1.1 General

Solar energy is a good and clean source of energy, which can help the world in experiencing the dirty and short of non-renewable resources, such as coal, etc. The country has accepted that the emission of greenhouse gases has led to increasing concerns about climate change. The department of energy (DoE) has developed a strategy in which the renewable energy sector can operate to grow and contribute positively to the country's economy together with global environment [7]. Induction cooking has been implemented long ago but lacking some advancement. The induction cookers in the market use mains power to operate of which limits the flexibility in terms of power sources. The working principle of the project is similar to what is in the literature, but with more of advancement features using auto selection in terms power sources, i.e. solar and mains AC power with the addition of battery storage as a backup and also to make it a complete portable standalone product. The benefits include economical, pollution free and sustainable energy conversion process as solar energy is adopted as the source.

1.2 Rationale for induction cooking system

The induction cooking system technology is one of the best cooking methods that have been developed up to date. The trending advantage includes high efficiency that is almost two times the existing technologies. The efficiency comes with low power consumption i.e. all power that is generated is transferred at least 80 % of the generated. The existing technology, electric stove and gas burners generate large amount of power in order to compensate for the power that is transferred to the surroundings in the form of heat. If taking a look at the research, as above induction cooking stove is the best cooking technology thus far. All of the above including induction stove is completely dependent into electricity generated by Eskom. The introduction of solar energy comes with the aim of filling the big gap existing amongst the use of electricity that is 100 % dependent on non-renewable resources. Below is the list of advantages and disadvantages of solar powered induction cooking system compared to the electric stoves.

1.3 Advantages of solar induction cooking system

- Reduce electricity bills
- Completely a standalone product
- The high harmonic semi-sine wave generated during induction process
- Easy to install
- Simple and reliable

- Safety
- Low maintenance
- No fuel cost and spills
- System can be made to be mobile
- High radiation index
- Auto power selection method (flexible in power sources)
- Sustainable development

1.4 Disadvantages of existing cooking technologies

- Dependent on non-renewable resources
- The cost of electricity bills and gas increases with resource demands
- Large amount CO_2 emission
- Electric stove is slower to cool down
- Electric stove may not work during storms (due to power outages)
- Gas is dangerous due to possibility of gas leaking
- Gas give off humid heat rather than dry required for effective roasting

The above advantages and disadvantages regarding existing cooking system compared with the proposed cooking technology create an improvement in cooking systems and it gives more options to the customer needs with regard to safety, ease to use, cleaning systems, conservation, and price.

1.5 Research objectives

1.5.1 General research objectives

The general objective of this research is to simulate and build a solar powered induction cooking system using auto selection method for any available power source, taking solar panel power as a priority for encouraging savings from using the grid power. Solar powered induction cooking system should be designed as a complete standalone product that is also portable and it can be used everywhere with the advantage of battery storage that is charged either by the panel or the mains itself if it happens the sun is not available for days. The aim also covers the reducing of electricity bills as the electric stove uses more power while half it is wasted as heat energy in the kitchen.

1.5.2 Specific research objectives

- Design and simulate an induction cooking system with eight programmed power levels.
- The design needs to accommodate calculations of the input power levels; half bridge, induction coil calculations, resonance frequency value, and pot resistance range of values and plot it in a graph for best pot material selection.
- Write a code to accommodate eight power levels and test it on the program script.
- Run the code on Proteus software and check for errors.
- Show each power level on the graph by means of PWM, load current and load voltage line graphs on oscilloscope.
- Design and simulate a charging circuit, AC to DC converter and charging circuit.
- Design and simulate LCD display for different power level and respective switching frequency.
- Build a DC to DC regulating system (MPPT) that is interconnected with the solar panels to monitor charging of the battery storage at 48 *V* and a maximum of 20 *A* charging current.
- Build an AC to DC converter that is fed from 230 *V* AC mains supply socket with an output voltage of 48 *V*, 10 *A* maximum to charge the battery and also be able to supply the half-bridge inverter circuit.
- Design and build a smart auto selection switch and connect it with the solar system and AC to DC supply.
- Build a charging control circuit for both solar and grid power.
- Build a half bridge inverter circuit with two N-channel IGBTs and design a induction coil and connect it in the middle of the IGBTs to form an induction cooker half bridge inverter.
- Build and program a power control circuit with eight different power levels corresponding with its switching frequencies.
- Test the Programmed LCD to display power levels as per the user selection.
- Integrate the whole system and demonstrate each and every power level with respect to the user selection.
- Test the auto selection switch, test if charging is working for solar and mains.
- Test the standalone feature for the cooker.
- Show graph of PWM, load current and load voltage and compare practical and simulation graphs.
- Overall design analysis, drawbacks, and future improvement suggestions for the continuation of the research.

1.6 Methodology

The design system is connected into two power sources, i.e. mains and solar (with battery storage assist system). The first supply of which is mains power is connected to an AC to DC converter (battery charger) of which is then interconnected with charging control circuit. The second supply solar panel is first connected with the DC to DC regulator, and then goes to the charging control circuit as well. The charging control circuit is than connected to the auto-switch circuit that directly feeds the half bridge inverter (induction cooking system). The induction cooking system is having input buttons for control purposes and according to the user need. The output of the cooker is having eight different power levels with different switching frequency.

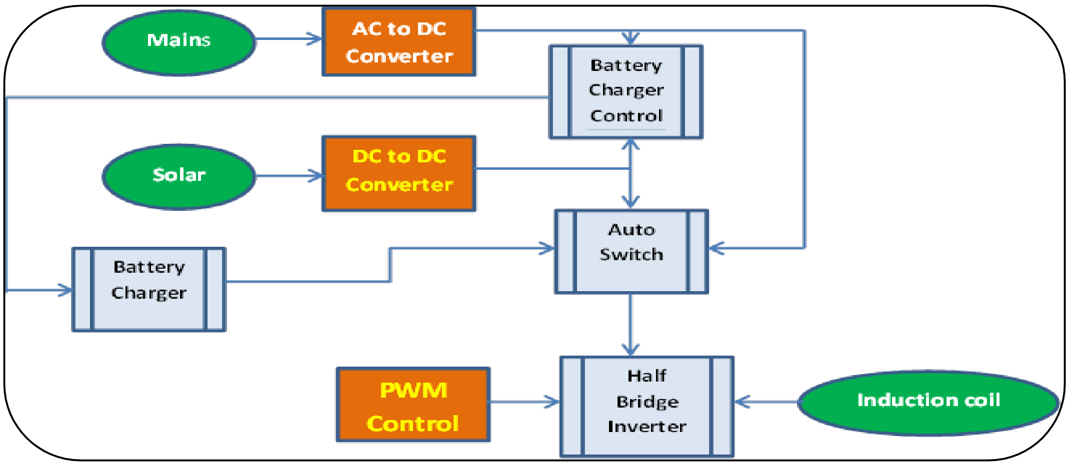

Figure 1: System block diagram

The above block diagram in fig. 1 shows all the stages of the design from two power sources (solar and mains) to the induction coil. The solar is taken as a priority in the power source selection as this is part of it advantage to promote free use of available energy from the sun. The design of each block is done using theoretical calculations and simulated in Proteus and Multism software packages. The theoretical, simulated results are compared with practical results obtained from the built system.

1.7 Contribution

Currently the country has developed the strategies by introducing a long term goal for renewable energy sustainability development in 2003 and wish to accomplish 42 % renewable based capacity by 2030 [7]. The use of renewable resources especially solar is always on the engineering articles nowadays. The funding for the renewable based research is all over the country as to meet the 2030 target.

All the research papers discussed in the literature in chapter two discusses about different methods to do induction cookers, the material of the coil, the distance between the coil and the pot and how the efficiency can be improved. All the cookers are power dependent to Eskom / mains power to operate and the cookers still utilise fossil fuels 100 % of which oppose what the country is looking to achieve. The power levels are few compared to the eight that are produced in this study. The focus on the previous study is more on being creative but not answering the country in terms of meeting the future goals / demands. The current method used in this study is similar to the existing study but putting improvement and also addressing the country problems by making it mains and renewable based. Mains power is still considered in the design since the country still consist of more fossil fuel based utilities. The research also contributes in the financial relief for high electricity bills from the home stoves. The research focuses in the theory, simulation and prototype building and testing of the induction cooking system.

The research is also more about making the cooker a standalone, completely independent from nonrenewable resources and smart in operation by being more user friendly and introducing more cooking levels to suit user needs. Smart cooking is introduced to improve the cooking in a more efficient and easy way by allowing the cooker to use solar energy as the primary source of energy and also be able to use mains as the alternative power source option. The cooker uses the auto selection of any available power source by doing the load power analysis and also in accounting for the savings (solar energy).

1.8 Chapter arrangement

The research content is organized in six chapters,

Chapter one: this chapter discusses about the history of the research on how it was done and how this present research is going to fill in the existing gap. This is explained by general and specific objectives of the research stated above. The chapter continues to show and explain the design methodology step by step to achieve general and specific objective of the research. This chapter also focuses on the contributions of this research on the existing research and how it will add a commercial value to the research.

Chapter two: in this chapter, induction cooking methods are discussed by explaining the major objectives and findings in each literature study presented and how it is related into this research by find the gaps in terms of the methodology used in the papers. The chapter also states how the gaps will be resolved in terms methodology, accuracy in findings and commercial value of the final product. The block diagram is explained in details by addressing the general and specific objectives of the research.

Chapter three: the design of the solar powered induction cooking system is presented in details by means of theoretical calculations and software simulations. The practical overall diagram is shown and explained in details by means of any adjustments made during the implementation section.

Chapter four: in this chapter, all the simulation and practical results are shown for each and every block in the block diagram that was presented in chapter three. The deviations or adjustments are explained in details.

Chapter five: The chapter focusses on the analysis of results and discussions. The results are analysed to explain if the general and specific objectives are achieved or not. The advantages and disadvantages of the design are discussed accordingly. The future of the research is discussed by means of suggested methods to improve the results.

Chapter six: this is the last chapter of the thesis. The purpose of the solar powered induction cooking system compared to the traditional existing cooking methods. Explain how the final results have overcome the shortfall of the literature explained chapter two. The methods used to achieve the general and specific objectives are discussed in brief. The quality and standard of the research is explained and together with the commercialisation of the product. The improvements are explained for future research opportunities.

1.9 Funding for the Project

This project has been funded by CSIR, UKZN from 2015-2017. The funding was granted to carry a renewable based project Solar powered induction cooking system. The funding has been granted for two consecutive years to further continue and complete the study.

2 Methodology

2.1 Introduction

Oil and gas are most commonly used fuels for power generation. Prices of such fuels are rocketing and the use of such fuels severely affects the environment. Global warming and green house effects are the main threat for the natural living system at the present situation and for the future generations [8]. Usage of fossil fuels for power generation is also one of the main causes for the environmental pollution. Sources which are environmentally clean, low in cost and easily accessible can serve the global community in a better way to save the environment. Solar power generation received significant attention due to many advantages such as less maintenance, no wear and tear and absolutely no cost for fuel apart from the factors discussed above. PV modules are used to generate electricity from sun [8]. Due to the non-linear characteristics of PV system, the output power is not constant all the times through the day. For the research, maximum power point tracking regulator is used to regulate the unregulated PV system.

Induction heating in nowadays is widely present in domestic appliances because of its cleanliness, high efficiency, safety and performance [2]. Induction heating is the process of heating an electrically conductive material (usually a metal) by electromagnetic Induction [2]. The time varying magnetic field around the conductor coil induces voltage and causes hysteresis losses as a form of heat when is exposed to a ferromagnetic material (pot) [4]. Induction heating allows high speed of heating and dissipation, all the heat produced is approximately transferred to the pot (greater than 80 % in efficiency) [1].

As presented above, solar and induction cooker provide cleanness and present high savings factor with regard to the use of massive free energy and high in efficiency by delivering more than 80 % of power output respectively. The high harmonics current generated from DC to AC conversion gives an advantage to the induction coil during coupling to give more current to the load and thus generate large amount power.

2.2 Literature survey

The analytical electromagnetic of domestic induction heating system is presented in [9]. The paper discusses about engineering principle of magnetic coupling between the system and the effect of it in the system operation together with looking at the mathematical calculations of the circulating currents and the contribution of it in the system load together with its amplitude to give rise to heating efficiency. The method and the approach used in the paper is similar lies within what is presented in all the literatures about induction cooking system. The paper touches important aspects, pot (load), coil and how the coupling affects the efficiency of the output power. The analysis is looking at the voltage and impedance matrixes and how these can give values of current and impedance in order to analyse induction system operation. The number of tests is performed in an experiment. The contribution comes with fact of getting to know how electric and magnetic currents describe the equation of potential balance of the system and how electric field and magnetic field can used to get self and mutual coefficients. The paper leaves a big gap in how the switching frequency is controlled, what method of switching is use either zero current switching or zero voltage switching, how the study can contribute to the community, only relies on one power source, no simulation study presented, et c. The study need to improve by addressing all above in order to promote research that will show how the study can be taken into practise to help our communities in the problems they facing. Taking note of the existing gap in the paper, induction cooking is now in the market and it efficiency, cleanness and safety is putting it as a number one stove compared to the ones existed long ago. Now the focus is to how the induction cooker in the market can be utilised in a more sustainable way by addressing the issues facing the country in taking renewable energy into practise as a DoE sustainability development. The study will design and build a portable solar powered induction cooking system that uses auto-switching method to make it flexible in terms of power sources by allowing it to be used either by solar or mains and it also present a battery storage that can be charged by both the power supplies, of which makes it a complete standalone which can be run without both power sources being available.

The design of zero voltage switching (ZVS) series resonant inverter is presented [10]. This paper touches very important sections for induction cooking system, i.e. influence of load, snubber circuit and dead time. The paper firstly discusses about ZVS of which is the method used in my study and it most in all the literatures, the method is very efficient and it increase the performance, it also cheap to construct. This study is also focuses in the efficiency of the induction cooker by looking at the existing traditional square wave (SW) modulation that operate in high frequencies to give low medium power levels. The proposed solution of this paper is to use a variable frequency duty cycle control to improve efficiency in the low and medium power levels by decreasing the switching frequencies. The gap still exists since it only focusses in the efficiency and in the parameters of the cooker to make it cheap and the best in the power output. This study does not answer the problem the country in trying to address in terms of how electricity that has been produced by non-renewable resources can be replaced in the future or either how it can be supplemented by the renewables as part of the sustainable development by DoE.

The solar-based induction cook top is discussed in [11]. This paper discusses about the solar powered induction cooking system. Each stage from solar panel, control circuit, battery, inverter and cook top is presented in details. The microcontroller and the LCD (liquid crystal display) for cooking level indications and control. The aim of the paper together with its conclusion was to implement a solar-based system with the idea of looking at the feasibility and advantage of using solar rather than electric or gas supply. The study proved that the installation can be costly but after 5 years, the user will be saving a large amount of *Rs* 12000. The study is in line with the goal of the sustainable development but lacking some advancement. The study did not consider the fact that the most of the country is currently running of Eskom electricity with the lack of renewable based capacity of which means it was going to be perfect if it considered the auto switching between the mains and the solar and introduce more power levels as to meet the user needs for different cooking stages. The idea of the paper was to compare the price savings that comes with the induction cooker compared to the gas and electric stoves. The study can be more improved if it can look at the real problem that is facing the country in terms electricity point of view.

The analysis of an induction-heating device with half bridge resonant inverter is presented in [12]. The circuit analysis and simulations of the inverter shows the eight function models of the circuit structure. The phenomenon of the skin effect plays a role in the analysis of the circuit. The study also look at the two factors that resulted in the temperature of the coil i.e. loss during current flow in the coil and the heat produced by the pot during operation. The paper focuses on the circuit analysis by looking into detail how the current flows in the circuit and how the same output current can be achieved using different material of heating coils of which is more of experimenting the theory learn in class rather using the theory into real life application by addressing major issues in the country into real problem solving. The study does not look into how the study can be utilised to solve the current cooking technology to it best. The paper is having great information that assisted the current study that I am doing. The information for circuit analysis and how many factors affect the operation of the inverter topology. The study can be improved by taking the theory and simulations that were performed into practise by looking at the existing gaps in research environment to address real life issues faced by the country.

The induction cooking assessment paper discusses about the comparison between the induction cookers, electric heating element stove and finally the gas burners [13]. The cooking efficiency ranges from 80 to about more than 90 % for the induction hob and about 50 to 74 % in electric stoves and lastly about 40 % in gas burners. The DoE after all the tests saw that induction cooking technology reduces the energy saving about 45 % compared to conventional electric stove [13]. This paper gives this thesis a go ahead and encouragement that the proposed solution of which addresses the efficiency improvement as discussed compared to the other cooking technologies, secondly addresses the issue of renewable based appliances as the country is aiming for the 42 % renewable based capacity by 2030.

Customer's satisfaction and attitude view amongst the induction cooking was done in city of Tirunelveli [14]. The study looks at the number of different induction cooking stoves since every company is marketing their cooktops with more performance and features. The preference and attitude is being investigated towards induction stove. The paper presents the advantages and disadvantages of advantages overcome the bad view of it. The level of satisfaction is about 80 % compared to the ones being dissatisfied. The relevance of the study with the current study comes with the fact that people are willing to invest in the induction cooking environment of which promotes the study in terms understanding the customer's attitude and satisfaction amongst the induction cooking technology that is presented in this research. The research takes this advantage and adds more features that will be in line with the country's goal for the sustainable development in the renewable energy sector. The journal does not focus in the power sources or in how the cooker is being powered but only look at the features like efficiency, safety, savings and etc.

The phenomenon of eddy current is widely understood since it explored in all the literatures [15]. Induction heating is highly used in industrial applications. There is also huge amount of work form academia and industry. This field is matured with a large number of innovative designs presented each year from academia [16, 17]. The FEM simulation model of conventional induction cooker is discussed in [18].This model focuses more on the two parts; namely wok and the coil. The modelled coil shows the even distribution of current in it. The overall simulation study conclude that magnetic field of the conventional cooker is uneven and localized which can lead to hot spot in the coil during operation and result in poor performance. The new method of changing the variable turn coil pitch by allowing the magnetic field to cover wide area improves the heating performance of the induction cooker. The overall aim of the paper was to emphasize and prove the importance of the variable turn pitch coil in the heating performance of the induction cooker and to investigate the structure together with problems associated with heating performance regarding conventional induction cooker in the point of magnetic field distribution. The effect of the pan material in an induction cooker and the topologies for an induction converter circuit is discussed in [19]. The comparison of the boost converter (quasi resonant) and resonant converter (half bridge) is studied. Five pans were tested. The frequency increases with the decrease in current and power proportionally. It concludes that pushing switching frequencies higher will reduce the cost of the coil, resonant capacitor, and increase the efficiency of the cooker. The induction cooker as a working electric transformer that generate heat on the secondary due to loading of the equivalent resistant of the losses is discussed in [20] The paper discusses in detail all the parameters from the coil to how the current density differs with respect to the number of turns in the coil. The modes of switching “hard switching” are studied in details showing how the power electronic device behaves under stressful switching. It also looks at the losses when the switch is exposed to high voltage and current at the same time. Snubber circuits assist in voltage transients on the switch during switching. The paper also focusses on the different topologies discussing the parameters in details. The simulations also support the theory in explanation. The control algorithm for both the topologies is discussed of which shows a slight difference between the two. The pan detection and circuit protection is presented in details in the flow chart. The practical discussion of the results corresponds with the simulations.

Currently the problem of trying to move away from non-renewable to more renewable based capacity still leaves a big gap in research as to how the country’s mandate for sustainable development in renewables be achieved. This study is part of the government strategies to increase the renewable energy capacity and also the renewable based appliances. The research will improve the annual saving by 45 % as per the DoE analysis in the comparison of cooking devices list in the Table 3 of paper [13].

In summary, most the papers discusses about the principle of induction cooking using mains as a supply and only few that discusses about the working of the cooker using renewable energy as a source of energy. The cookers on market on the research as the above focuses more on the pan material and on how it affect the performance in terms of heating the coil and producing more electric field. It also covers more deeply in the switching frequencies and on how changing the frequency can be done using power electronic switches. The protection also plays a vital role since the generated magnetic field can cause such high currents in the plate. Topologies are discussed in all the literatures and all the conference papers. The topology selection is very important as they all play different roles with respect to efficiency and cost effectiveness. The study on this research is a solar powered induction cooking system that works in a similar manner using the principle of magnetic fields induction to cause eddy current to flow in a ferromagnetic material resulting in heating. The study focuses also on the auto switching method for selection between two-power source, namely solar power and mains AC power. The auto selection is to select any available source of power between the two. The cooker uses the batteries that is to be charged by both solar and mains but treating the solar as a priority always in order to promote the use of free energy when it available. The cooker also work with batteries alone of which makes it completely portable and being a standalone product that can work for about 4 hours without solar and the grid being present at the time. In this research, the simulation study is done for testing the heating level at different frequencies. The practical implementation using solar and mains switching is also shown in the implementation section.

2.3 Research methodology

The flow chart diagram in the Fig. 2 below shows the power flow of the system in detail. The chart shows how the interface responds to the user selection. The system consists of an LCD display to indicate power level and switching frequency and also gives the system status for any user input. The program in the flow chart first asks the user to select desired power level. The selected power will send a specific signal to the system and the system will do a power analysis to check if the battery power is enough to supply the system. If the battery is not enough, the system will automatically switched into mains supply. After the cooking is done, the mains will than charge the battery.

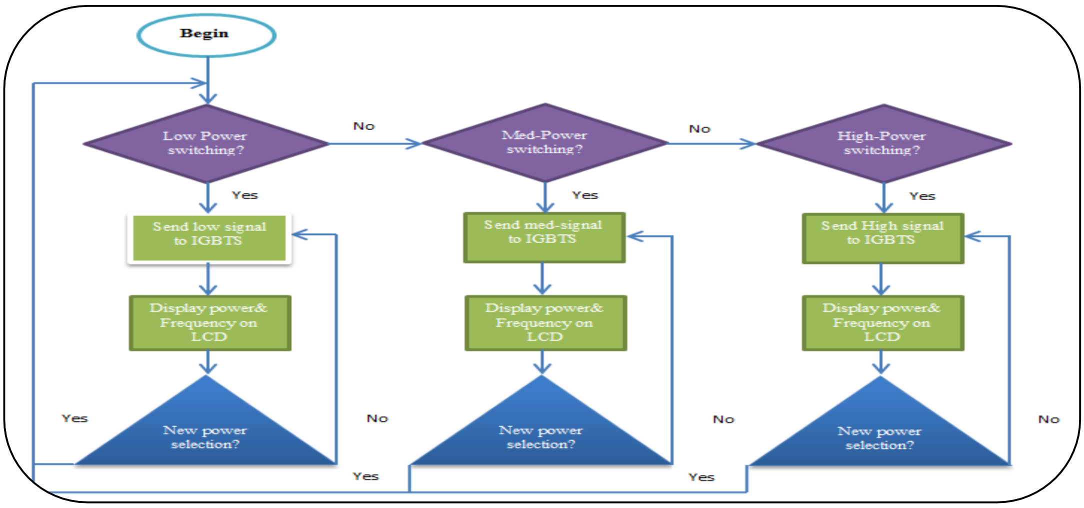

Figure 2: Design power flow chart

The design consists of two power sources, i.e. solar and mains power. The two power sources are connected directly to the system. The mains power provides with +/- 230 *V* and that is converted into direct current via the converter since the system requires direct current input. The converted DC voltage is 48 V that is able to charger the battery storage and also be able to independently supply the system. The converter is connected with the first section of the battery charger control circuit for mains supply charging. The second section of the charging circuit is the MPPT regulator that is connected to the solar panel, if solar is selected to charge the battery instead of mains. This means that the battery storage can be charged either by solar or mains power but treating solar a priority power source. The MPPT is design to regulate the unregulated/ fluctuating DC voltage from the panel. Two panels of each 300 watts are used to provide a maximum of 600 watts. The user interface with the buttons is designed for the user to be able to select any power level required. Each power level is programmed with a specific switching frequency. The switching frequency is controlled by means of the duty ratio. Each complete circle of the pulse width modulation (PWM) is accommodated with a switching dead time of +/-5 % to allow the switches not to switch at the same time as this might result in a short circuit. The switching method used is zero voltage switching (ZVS), i.e. no voltage will be across the switches during the switching. The ZVS is achieved by switching at frequencies higher than the resonance frequency.

2.4 Design stages

2.4.1 Stage one

The first step is looking at the theoretically study by drawing each circuit for a specific block in the block diagram shown in chapter one. After the circuit analysis is done, the theory is translated into mathematical calculations for each component to be used in the design.

2.4.2 Stage two

The theory and calculations is now taken into software for simulation analysis. The simulation study is to indicate if the proposed circuits together with it calculations can be simulated and compared with what is in the theory. The graphs are shown and the values are tabulated accordingly.

2.4.3 Stage three

The simulation study is now taken into practise. The feasibility of each circuit in the block diagram is designed and tested if it corresponds with what is in the theory and calculations.

2.4.4 Stage four

After each circuit in the block diagram is achieved in the form of implementation, the integration of the whole circuit is tested and the results are recorded. All the recorded results are compared with what is in the literature and what is in the general and specific objectives of the research.

2.4.5 Stage five

This stage presents the overall results analysis and discussion, providing detailed explanation how the completed product will address all the issues mentioned in the literature by looking at the financial point of view, savings and its efficiency. The standalone feature is tested in this stage.

2.5 Conclusion

To conclude, the country is investing a lot in renewable based research in aiming to address the current issues with regards to electricity price, demand, and toxic gases released by non-renewable resources. The literature presents the existing research that is addressing many areas regarding induction cooking technology. This specific research is aiming using the literature to address the issue of relying more in non-renewables and trying to help the country to achieve its on-going of renewable sustainable development. At this stage of the thesis, the confidence is 80 % that the design will successfully address all the mentioned missing improvements in the existing literature.

3 Design of solar powered induction cooker

3.1 Introduction

Solar powered induction stove is about to improve the annual cooking energy costs about 45 % as discussed in the literature chapter II. The solar induction cooker presents cleanness, high savings with regard the free energy from the sun and lastly by delivering more than 80 % efficiency in terms of the power output. All the facts has been gathered from first and second chapter on the research about how solar can be of good and reliable source of supply for domestic applications as the country is facing utility power issues with regard to the load shedding Problems as a result of planned and unplanned load-shedding that cause inconvenience. The cooker as reliable product present features like, battery storage as a backup that makes it a completely standalone product in the case solar is not available at the time. The theory of the design has been explained in detailed from the first two chapters including the general and specific objectives of the research. This chapter combines all the general and specific design objectives into reality in terms of performing relevant calculations and simulation models for each block in the block diagram explained in chapter one. A pulse width modulation technique is used to control the cooking power levels as per the user input. The below section concentrate more on the mathematical and schematic design of the design.

3.1 Design of solar powered induction cooking system

The block diagram below in Fig. 3 shows the overview of the design stages by indicating the important blocks that plays a vital role in the circuit operation. The power flow is indicated by the arrows, showing how the communication between the blocks is conducted respectively. The design consists of two power sources, i.e. solar and mains power. The solar panel is having PV solar cells that convert light energy into electrical energy by means of direct current. The converted DC value depends on the amount of light intensity as to how much it can extract from the maximum power a panel can produce. The two panels of each 300 watts are combined to make 600 watts maximum. The panel voltage and current are having non-linear behaviour since their output is unregulated. The solar assist function (MPPT) is initiated to assist the power control from the panel to the battery for charging. The MPPT function will buck and boost the voltage and current to meet charging demand of the battery unit. The battery unit is 48 *V* and 25 Amps in capacity. The MPPT makes sure that the battery is charged and discharged accordingly, as to lengthen the life of the battery unit. The regulator unit has fast charging capabilities to make sure that battery is charged at it fastest rate. The regulator is than connected to the relay interface. The relay interface communicate with both the power sources by making sure the power flow is from the correct source at a specific time. It also makes sure that there is no reverse power flow and that solar is the main power source for the cooker while the mains are a backup source. The relay is the mind of the system and every decision it takes is initiated by the circuit breakers. The relay contacts are connected such that if the solar power is immediately disconnected or there is no enough energy to supply the battery unit, the relay checks if the battery power is still enough to provide power to the cooker. Thereafter the relay will make a decision as to close the relevant circuit breaker to check and allow the mains to take over in powering the cooker. At the same stage, the relay will close another breaker to make sure that the battery is also charged by the mains for it to remain full. The second power source is of which is mains is connected to AC to DC converter to produce the same voltage for charging and for supplying the cooker directly. The converted DC from the mains will sufficiently supply both the battery and the cooker at the same time. The half –bridge cooktop is the main receiving end of the design. The cooker only seat and wait for the user input, thereafter it sends a message to the relay asking for the power availability. The relay will then do the above mentioned steps to check for the best suitable power source depending on the availability and user power level demand.

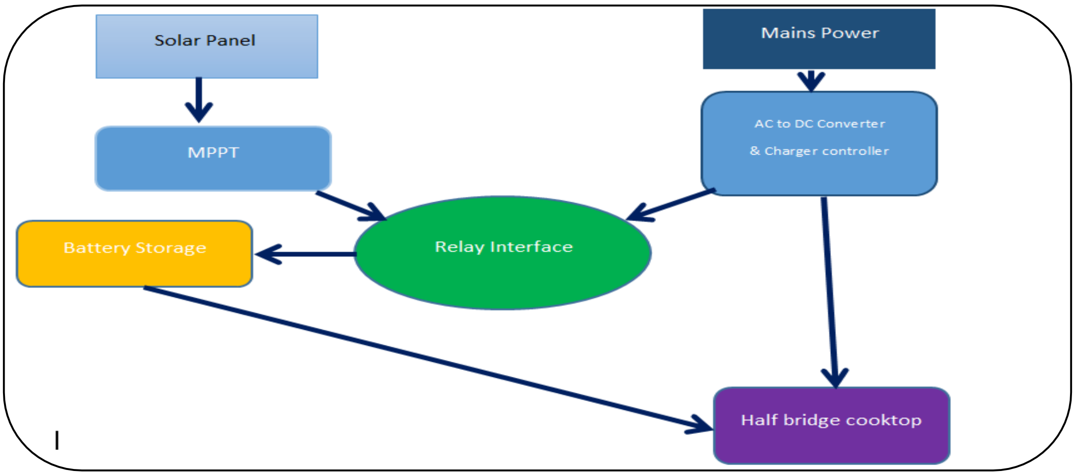

Figure 3: Design block diagram

3.1.1 Solar panel and MPPT

The PV system converts the solar radiations falling on the PV panel into electrical energy. The converted energy is directly proportional to the amount of sun's radiations received by the panel at a specific time of the day. Two solar panels are connected to give a maximum of 600 watts of each contribute 300 watts maximum. The system is designed to charge a 48 *V* battery 25 *Ah* in capacity. The solar is the primary source of supply for the cooker. Solar is made up of photovoltaic cells that converter solar energy into electrical energy in the form of direct current [21]. PV modules generate electricity from sun [20]. Due to the non-linear characteristics of PV systems, the output power is not constant all the times throughout the day. In this design, batteries, maximum power point tracking function work together with PV systems to regulate the voltage of the PV systems. In this research, solar is the main source power for heating the induction coil and 300 *W* solar panels are used. This unit depends on the sun radiation to supply energy but using battery storage for stability. Below are the theoretical calculations for the design of solar panel system. Firstly battery capacity is 48 *V* and 25 Amp Hours (*AH*). The conversion of *AH* into watts is required and the conversion can be seen below;

$$P_{available} = AH \ x \ V_{battery} \quad (1)$$

- *AH* = Battery size
- $V_{battery}$ = Battery Voltage
- $P_{availavle}$ = available power in watts hour (*WH*)

$$P_{available} = 25AH \ x \ 48V = 1200 \ WH$$

The equation above shows that 1200 *W* of power can be supplied for 1 hour, and 600 *W* in 2 hours etc. The energy intake is proportional to battery discharge. The amount of power in a battery (battery size) can be always adjusted, 48 *V*, 25 *AH* battery is used for research purposes only. Though the rule of thumb says battery can give as much as 50 % of its capacity as there is a drop in voltage as power is dissipating. The amount of power the panel can give to the battery is calculated as 2 x 300 *W* panels multiply by the average hours of the sun during the day. South Africa receives huge amount solar radiation ranges between $16.2 \ MJ / m^2$ *to* $23.4 \ MJ / m^2$ per day [22]. The average amount of sun in Kwa-Zulu Natal is 6.5 hours and the charging amount can be calculated as 600 *W* multiply by 6.5 hours to give 3900 *W*. This means that the system can charge the battery to its full state three times in one day.

3.1.2 DC to DC regulator

Fig. 4 shows the simulation diagram of the implemented scheme. In the proposed simulation study, both MPPT and output DC voltage regulation are carried out. Regulation is needed to provide constant voltage at all times as solar output fluctuate all the time.

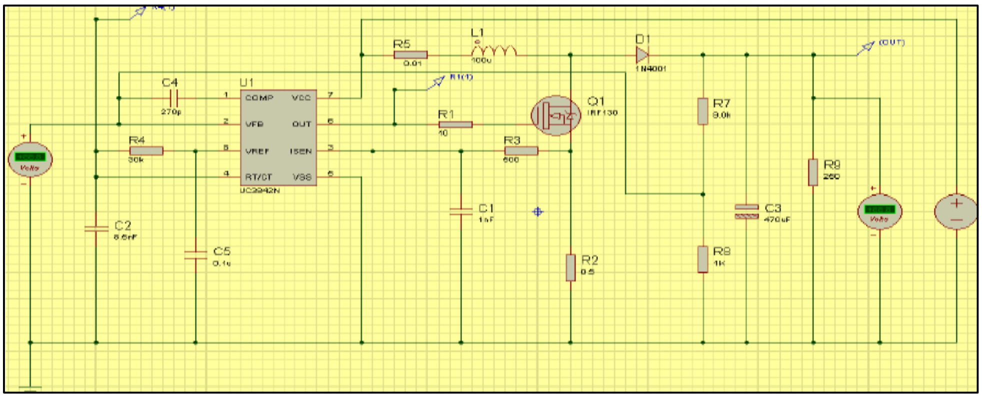

Figure 4: DC to DC converter

The converter regulates the unregulated DC supply of the solar panel. The smooth DC supply is necessary for the charging unit to be regulated DC for charging purposes and to supply the inverter with smooth supply. 75 *V* DC to 48 *V* DC converters is used in the simulation. The solar voltage is 37.5 + 37.5 *V* DC and at 8 *A* maximum. The regulator will then convert the 75 volts from the series connected panels to 48 volts to match the system requirements.

3.1.3 Mains

The mains power is directly connected to the grid. The need for the mains power is to provide backup system for the design and to make the product more user friendly in terms its flexibility regard power sources. The grid is directly connected to the system via the AC to DC converter. The grid provides +/- 230 *V* AC and that is converted to 48 *V* DC to meet the system voltage specification. The converter is charging the battery storage at 48 *V* DC. The mains play a role only if the solar cannot provide enough charging for the battery storage. The grid will charge the battery using the converter and also it can directly supply the cooker during the times of no solar available for a long period. The smart programmable relay is used to do the automatic switching in the above given cases.

3.1.4 Auto Switching / Relay interface

The auto select switch makes the auto selection of any available supply between solar and the grid and select whichever is sufficient by doing power demand analysis. The solar power is priority in the analysis for cheap selection and usage. In simulation, the auto switch is controlled by microcontroller program. The battery power level is compared to the switching state selected. If the battery level is sufficient the coil is powered from the battery. In this design, the auto switch is programed such that the source selection is done at the beginning of each cooking state. If the battery is not sufficient to supply the required power for the cooking state selected and for the duration calculated, the mains power will be selected and the battery will be charged either from solar or from mains. In this section smart programmable remote relay will be used in the practical section to make things easier for the implementation due to time frame. The relay switch act as the load shed controller, day night switch and a solar assist function.

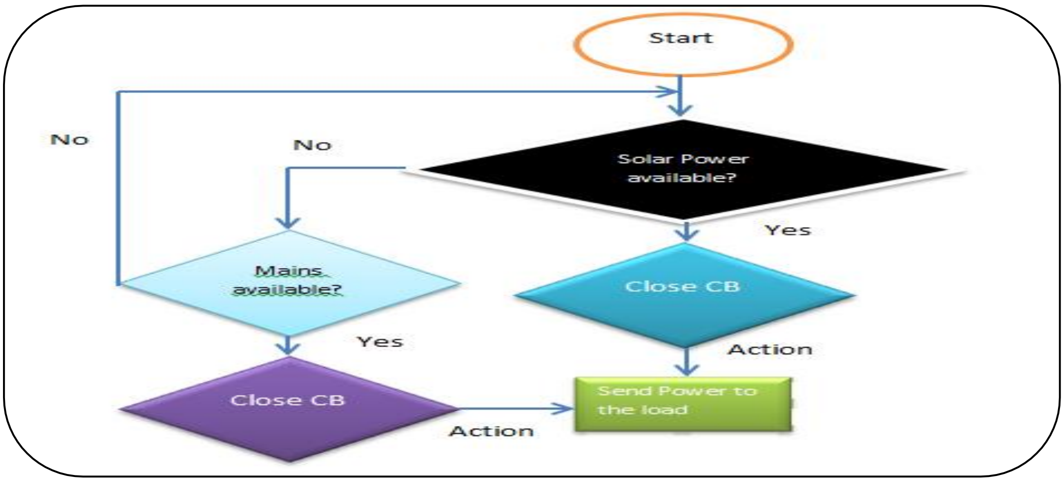

Figure 5: Relay interface internal feature

The flow chart in Fig. 5 above only show the specific actions for it purpose in the auto selection. The relay is programmed such that from the beginning it asks if the solar power / battery are available. If the solar / battery is available and enough to supply the load, the circuit breaker (CB) is closed such that power flow from solar system to the load. In the case that the solar systems have no power, the second step is to check for the backup power (mains). If the mains power is available, it respective CB will be closed by the relay signal allowing power flow from the mains to the load. If the both power is not available, the relay will keep on checking for the power availability by following the same flow as explained and indicated in the diagram above.

3.1.5 AC to DC Converter

AC power is commercially inexpensive and easily available while DC power is expensive to generate. However, rectifiers are used to convert the readily available AC power to DC [23]. Rectifiers produce DC voltage with very high ripples and filters are required to smooth the DC to around a constant value [24]. The filters are divided in inductor, capacitor and capacitor – inductor filter. The filter selection depends in the application. The capacitor filter is for low, inductor for high power applications [25]. The mathematical expressions for capacitor and inductive filters do exist [25]. The DC is having three types of rectifiers namely, half-wave rectifier, full-wave rectifier and full-wave rectifying bridge. The Fig. 6 below shows the AC to DC scheme.

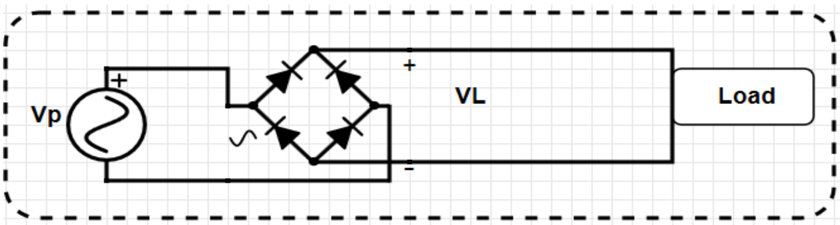

Figure 6: AC to DC scheme

Considering the AC input voltage as sinusoidal. The full-wave rectifying bridge is selected as it more advantageous compared to the other ones. The load voltage and current are defined by the equations below;

$$V_{dc} = \frac{2.V_S}{\pi} \quad (2)$$

$$V_L = \frac{V_S}{\sqrt{2}} \quad (3)$$

$$I_{dc} = \frac{2.V_S}{\pi.R_L} \quad (4)$$

$$I_L = \frac{V_S}{\sqrt{2}.R_L} \quad (5)$$

The mains source voltage is taken as 220 volts from the AC socket for calculations and simulations (see appendix A). Equation 2 is the expected DC voltage at the output, eq.3 is the load voltage and eq.4 and 5 is the DC and load current equations respectively.

The mains power is an alternating current while the system requires direct current supply. AC to DC conversion is necessary for the design as above. The converter will be able to charge the 48 *V* batteries and also supply the load direct in case the solar power fails. This part of the thesis is not designed from first principle but the converter will be ordered using the solar panel specification in section 3.1 above. The charger will charger as fast as the solar panels.

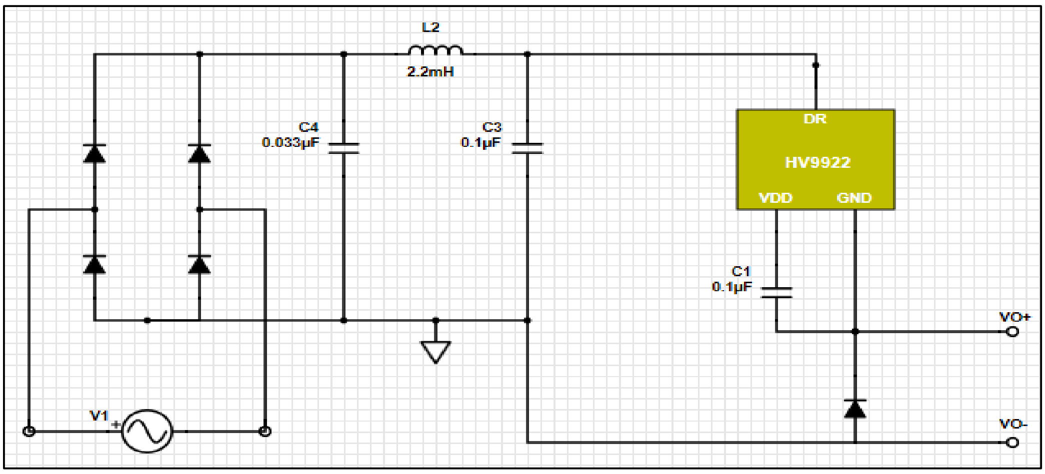

Figure 7: AC to DC power supply

The above Fig. 7 is the simulation schematic of the AC to DC power supply. This converter makes it convenient for the batteries and the half bridge converter to work perfectly since the implementation needs only DC supply. 220 *V* AC is converted to 48 *V* DC at 542 *W* power level. The other most important factor is to make it flexible in the range of frequencies for different power levels in the inverter section.

3.1.6 Battery storage

Energy storage in history has reflected as the most complex issue in the industry applications. It presents the independent feature as it can be used in standalone products or applications [27]. Below are different types of batteries and their theoretical explanation;

3.1.6.1 Primary Batteries

Primary batteries are defined into standard zinc-carbon and alkaline or heavy duty [28]. These batteries present a convenient power supply for all the electronic devices, hearing aids, toys, memory backup etc. providing relief from utility power. Their advantage comes with the easy to use, reliability and acceptable cost for the poor. In Table 7.1 different characteristics and applications of primary batteries are shown in [26]. Their stored electrochemical power cannot be reversed by means of charging after use. Zinc-carbon cells are the cheapest kind of primary cells though their voltage per cell ranges from 1to1.5 volts while the alkaline have a better capacity and thus having a long life (heavy-duty) [28].

3.1.6.2 Secondary Batteries

The secondary batteries are divided into nickel-cadmium and lead-acid [28].These kinds of batteries are rechargeable and they are the most used in many applications around the world. Their use comes with starting, lighting and ignition automotive and also their recent interest presents power supply for hybrid and electric vehicles [26]. It is major used in two different applications namely, as energy storage to deliver power on energy demand and it is charged by the primary energy source to keep it in fully charged state. The second major application comes with the discharged and recharged after use. The charging and discharging presents a convenience in cost savings as it can be recharged instead of being replaced [28]. Lead-acid batteries can be classified into automotive, deep-discharge or traction, stationary, low-antimony solar battery and sealed or valve regulated.

3.1.6.3 Selected option for design

The selection for storage method is based on the design specific objectives. The design is based on secondary batteries as they present the rechargeable characteristic. Lead-acid batteries are selected for the design as they have solar based batteries under their categories. The solar batteries present a fast charging and long discharging of which is required in the design to long last in the case of demand (no mains supply). The graph below in fig. 8 shows lead-acid battery categories.

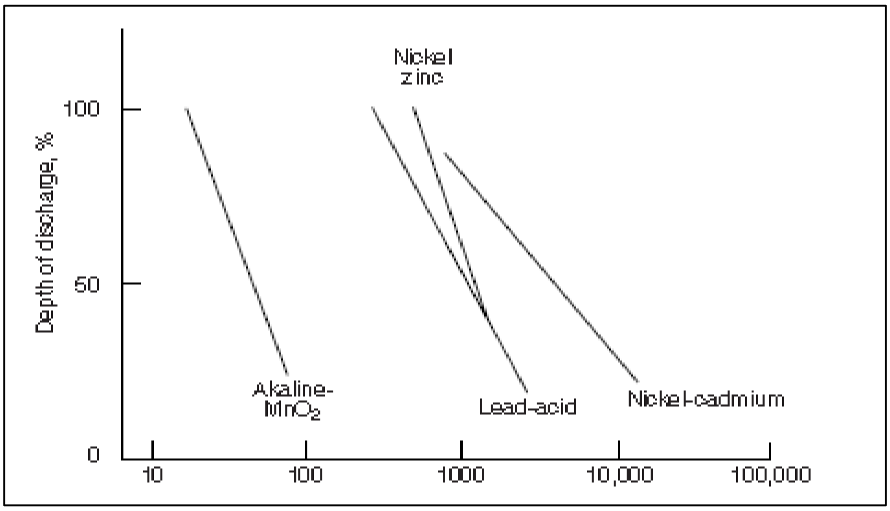

Figure 8: Cycles life versus depth of charge for several types of lead-acid batteries [26]

As it can be seen in Fig. 8 above, the low-antimony solar batteries show a low distilled water consumption and low discharge rate. Their cycle ranges from 1200 to 3000. The disadvantage comes with the expensive cost but it can be compromised as their life cycle is huge compared to the less expensive of which than works the same price if not less. The last advantage is that they don't need too much maintenance compared to the other types of battery storage. Solar rechargeable batteries are the ones to be used in the design since they provide reliable system for PV systems. The chosen battery capacity is 48 V 25 AH as indicated in section 3.1. Section 3.1 also shows the equations on how long it takes to charge and discharge the storage system chosen.

3.1.6.4 Battery charger simulation circuit

The battery charging circuit is divided into two, first section is the one connected directly to the solar panel via MMPT regulator and the second section is the one connected to the mains via AC to DC converter with its charging control unit. The Fig. 9 below shows the simulation circuit for the battery charging unit. The battery chargers are auto-configured, i.e. they communicate accordingly on who must operate at a given condition at a specific time. The battery storage is charged at 48 *V* DC and is disconnected if an overflow of voltage occurs in the system of which will be indicated by different lighting indicators on the implementation section of the design.

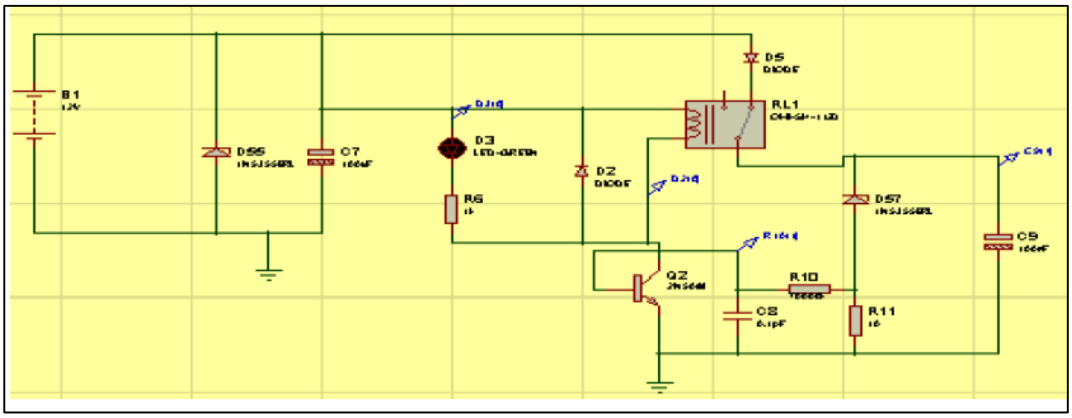

Figure 9: Battery charger circuit simulation

The battery storage is for energy accumulation that has electrochemical cells. Portable size solar rechargeable batteries are used in order to maintain load levelling. The charger controller circuit controls the charging and the discharging of the battery level to extend the life of the batteries.

3.1.7 Half bridge cooktop

This part of the design is the heart of the whole system. The power flow and heating levels are channelled through the switches (IGBTs). The circuit is connected to the DC power with two switches at the open state. Below Fig.10 is the model circuit;

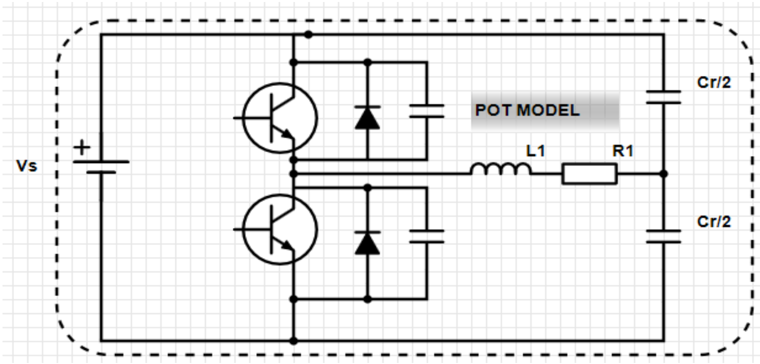

Figure 10: Half bridge inverter model

Fig. 10 above shows the model of the cooker. The two switches are switched alternatives to change the DC into high semi-sine wave frequency alternating current. The two capacitors provide the continuous power flow during the dead time in the switching.

3.1.7.1 Circuit analysis

The single phase half bridge inverter circuit provides a cheap and easy circuit to construct while also it more efficient in terms of the energy losses as it only contains two set of switches [29]. The circuits in Fig. 11 below shows the analysis of the half bridge topology used in the design.

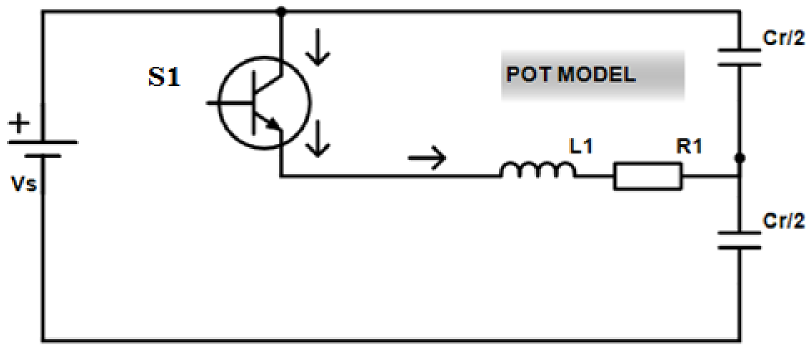

Figure 11: State 1

V_S is the DC voltage supply with the two switches connected together. The blue arrows in the figure above show the direction of current flow during state 1. The blue arrows show that load current is positive and it is supplied by the high side transistor.

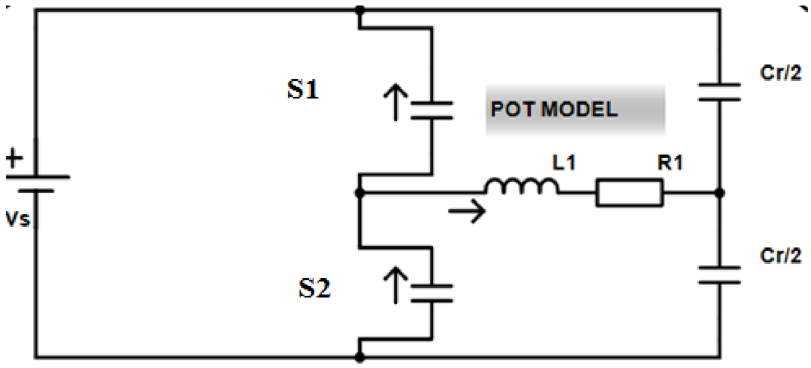

Figure 12: State 2

S1 is switched off, the resonant current flows through and charges or discharges the snubber capacitors and thus the low side capacitor is discharged while the high side capacitor is charged.

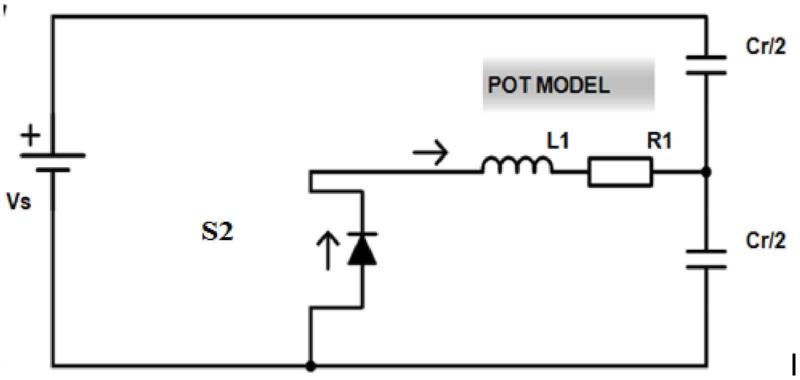

Figure 13: State 3

S1 resonant current starts free-wheeling the low side diode (S2). The load current is still positive.

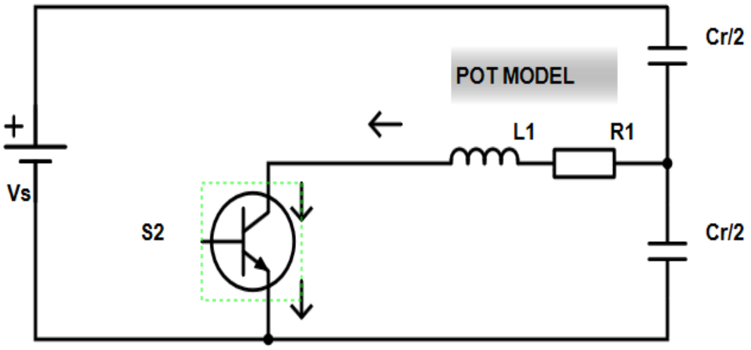

Figure 14: State 4

S2 is turned on, the load voltage turns negative when the low side transistor is turned on (S2), as it can be seen by the flow of current (blue arrows).

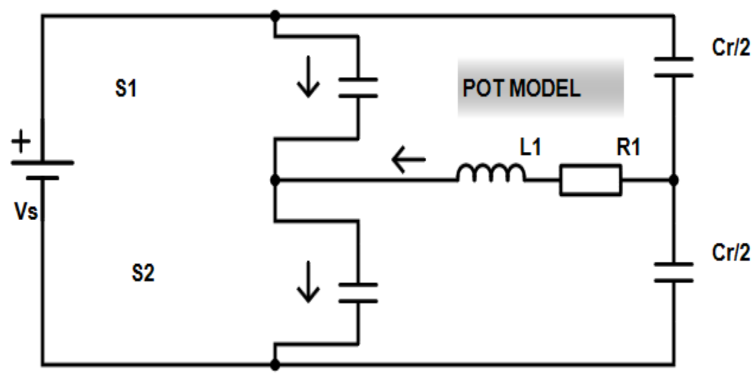

Figure 15: State 5

Low side transistor is turned off, load current charges S2 snubber capacitor to supply voltage while S1 snubber capacitor is discharged simultaneously.

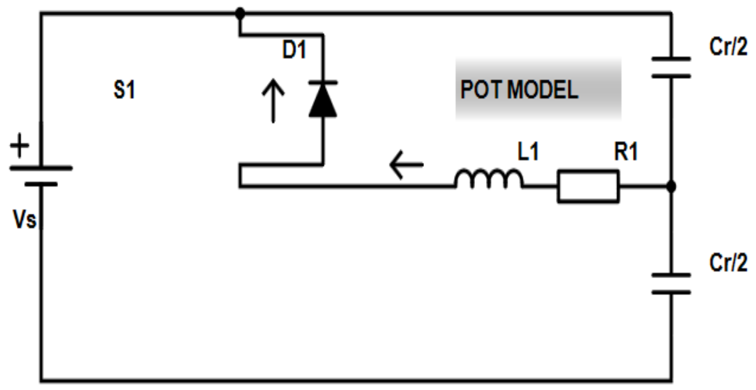

Figure 16: State 6

When both capacitors are charged and discharged the negative load current flows through the high side diode (S1). When load current approaches zero, the system start again from STATE 1.

3.1.7.2 Snubber Capacitor

The snubber capacitor reduces losses during switching of the transistor. During the on state of the transistor, the diode is off and all the load current flow in the transistor. When the transistor reaches source voltage, the load voltage goes to zero. After transistor voltage matches source voltage, diode current increases to load current and the transistor current goes to zero. As a result, there is a state where both transistor current and voltage becomes high at the same instance, resulting in a triangular shape instantaneously as seen in the figure below. The snubber provides another path for the load current. The rate of change of the transistor voltage is minimized by the capacitor, delaying its voltage from high to low transition.

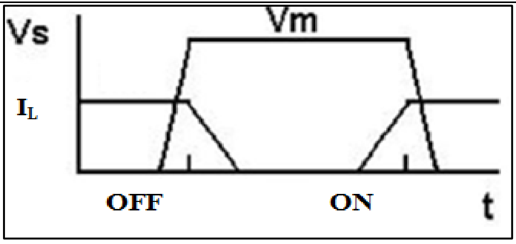

Voltage and current during switching

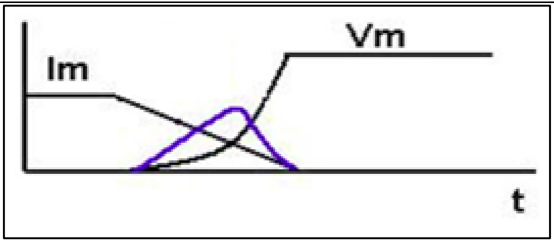

Turned off waveform with the snubber capacitor

Figure 17: Snubber circuit

3.1.8 Power flow control circuit

This section is connected together with the user interface. The input for cooking power level is control via buttons that are connected to the power flow circuit. The user presses any power level on the buttons and the load power demand analysis is done to make sure if the power selected is available at the time. If the power is not available, the message will be displayed on the LCD stating the issue or else the selected power will be sent to the half bridge and displayed in the LCD together with the switching frequency.

3.1.8.1 Design

The design of the half bridge inverter has two important parameters for the design attention needed to be carefully studied. It is the value of the resonant capacitor tank and the inverter switching frequency.

In the half bridge circuit (RLC), resonance is a result of the collapsing magnetic field of the inductor that generates an electric current in its windings which charges the capacitor while the discharging capacitor provides and electric current that builds the magnetic field in the inductor. The resonance occurs at a particular frequency for a given values of capacitor and an inductor. The highest electrical power and efficiency is produced at this stage of resonance. The half bridge switching frequency selection is very important and is dependent on the value of the resonant capacitor and by extension the resonant frequency. The half bridge will operate under zero voltage switching condition (ZVS). ZVS is when the voltage across the switch is zero when turned on (there will be current flowing through the body diode of the switch). The above is achieved by switching the half bridge at frequencies higher than resonant to maintain this state safely.

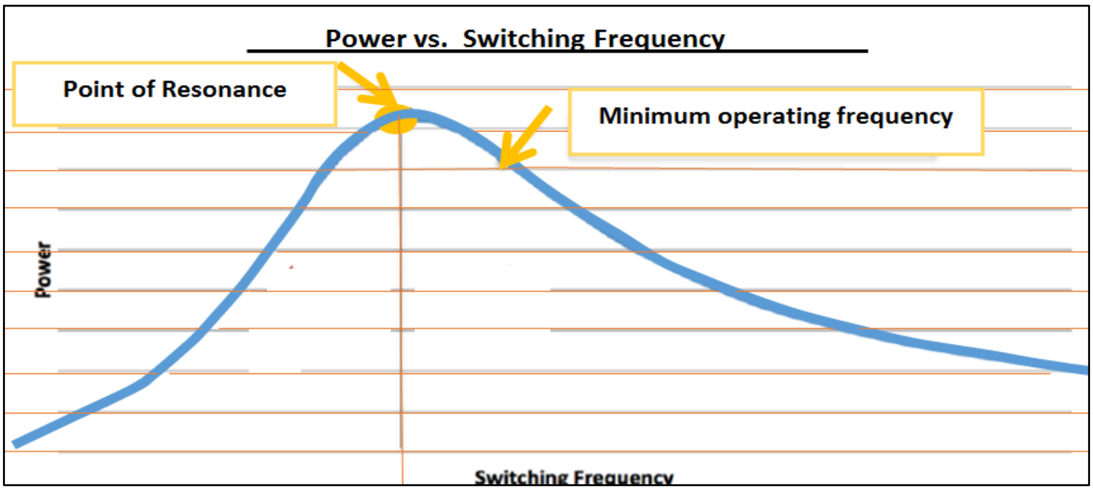

Figure 18: Operational range of the half bridge

The Fig. 18 above shows the resonant frequency is the point of maximum power. Frequencies lower than resonant are in the zero current switching (ZCS) domain. Since capacitors and inductors have the capacity to vary slightly from their rated values especially during the use, it is necessary to operate in the ZVS territory with some factor of safety.

The output power, P_h for the harmonic (h) in the inverter can be determined using the Fourier transform as in the equation below.

$$P_h = V_{h,rms} * I_{h,rms} \quad (6)$$

Impedance, Z_h in the circuit is defined using the equation (7) in fig. 19 below. Where, $R_{eq}$is the equivalent resistance of the pot, the inductive reactance? $X_l = \omega L$ And the capacitive reactance $X_c = \frac{1}{\omega C}$.

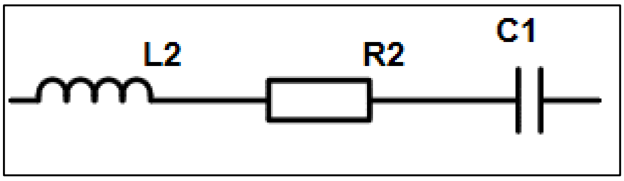

Figure 19: Circuit impedance diagram

$$|Z_h| = \sqrt{R_{eq}{}^2 + (\omega L - \frac{1}{\omega C})^2} \quad (7)$$

$$\omega = 2\pi f \quad (8)$$

$$|Z_h| = \sqrt{R_{eq}{}^2 + (2\pi f L - \frac{1}{2\pi f \omega C})^2} \quad (9)$$

Current, $I_{h,rms}$ in the circuit at harmonic (h):

$$I_{h,rms} = \frac{V_{h,rms}}{Z_h} \quad (10)$$

$$I_{h,rms} = \frac{V_{h,rms}}{\sqrt{R_{eq}{}^2+(\omega L-\frac{1}{\omega C})^2}} \quad (11)$$

The overall equivalent resistance, R_{eq} of the circuit can be defined as fellow; Fig. 20 gives the relationship between the equivalent resistance and switching frequency.

$$R_{eq} = R(f_s)\frac{f_s}{fr} \quad (12)$$

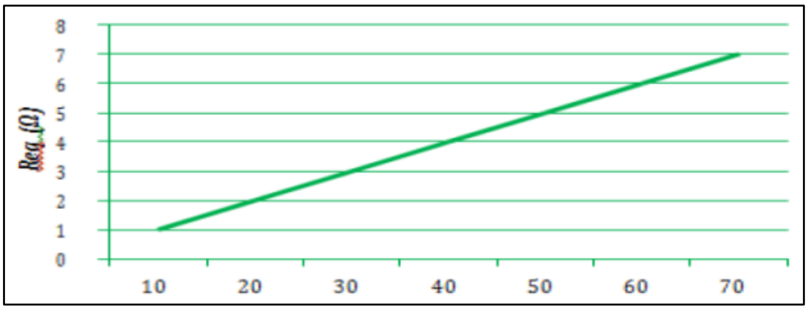

Figure 20: Dependence of resistance on switching frequency

At resonant frequency, the impedance only shows resistive component as the inductive and capacitive reactance of (7) becomes equal. Therefore the resonant frequency of the circuit can be calculated as below;

$$f_r = \frac{1}{2\pi\sqrt{LC}} \quad (13)$$

By manipulating equation (8) using Ohm's law and by filling in known variables, a solvable equation for the harmonic (h) power output can be derived (16).

$$P_h = I_{h,rms}{}^2 x R_{eq} \quad (14)$$

$$P_h = \frac{V_{h,rms}}{\sqrt{R_{eq}{}^2+(\omega L-\frac{1}{\omega C})^2}} x R_{eq} \quad (15)$$

$$\Sigma h = 1P_h = \frac{\frac{2R_{eq}V^2{}_{mains}}{(h\pi)^2}}{R_{eq}{}^2+(2\pi f L-\frac{1}{2\pi f\omega C})^2} \quad (16)$$

The resistance is selected according to pot material and resonant frequency of the selected choice. The graph in appendix (B) shows the resistance of the pot material with respect to it resonant frequency. The cast iron material is selected and the corresponding resistance with respect to the chosen resonant frequency is 1.8 Ω. The iron is chosen over aluminium due to a very high resistance at 10 kHz. At 10 kHz aluminum resistance is at 0.2 Ω while cast iron is 1.82 Ω. The inductance of the coil is chosen to be 99 uH and the resonant capacitance will be calculated from this value of the inductance using equation below;

$$f_r = \frac{1}{2\pi\sqrt{LC}}$$

$$C_r = 2558\ nF$$

Table 3-1 gives the circuit characteristic for the design of the induction coil and the load using resonant estimation calculation;

Table 3 -1 : circuit parameters

Parameter	Definition	Calculated value
L_{eq}	Pot coil inductance	99 uH
$R(f_s)$	Induction pot resistance	+/-1.82 Ω
C_r	Resonant capacitor	2558 uF
h	Harmonic number	1
f_s	Switching frequency at maximum power	10 kHz

Using equation (12) and (16) the graph below is generated to illustrate how the output power varies with frequency.

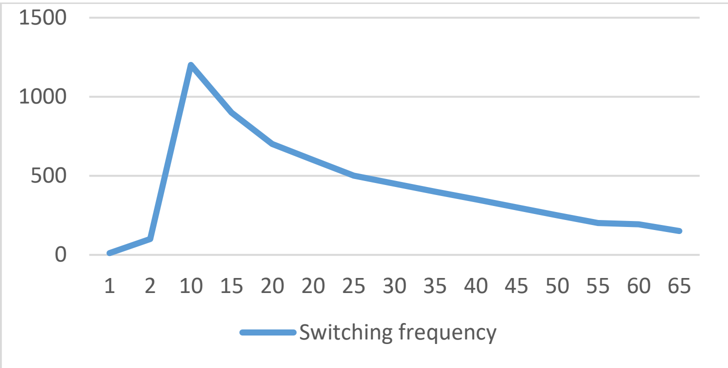

Figure 21: Output power vs. Frequency

Fig. 21 above shows that the peak power is achieved at resonant frequency, 10 kHz. It is important to choose a frequency a bit greater than resonant in order to approximately achieve zero voltage switching, meaning that the switch is opened with zero voltage across it. During this switching the circuit will consume 1200 W.

3.1.8.2 Simulation diagram

The advantage of using half bridge is that the high frequency harmonics can be utilized to produce heat in the coil. The simulation design of half bridge circuit with cooking coil is shown in Fig. 22.

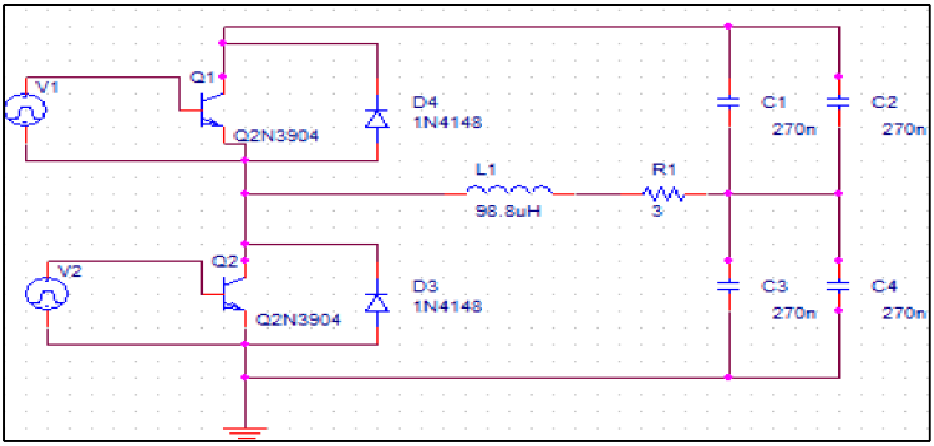

Figure 22: Half bridge inverter with the cooker coil

The half bridge circuit is designed to convert the direct current from PV and mains to alternating current. The half bridge circuit shown in Fig. 22 is designed using two IGBTs to convert DC into AC. A 48 *V*DC is fed to the two IGBTs which are converted to an alternating current by sending opposite PWM signals to the switches. The amount of voltage created on the coil depends on the switching frequency and the pot material used. The power ranges from 100W to 600W. L1 and R1 represent the cooker coil and the pot respectively. The four capacitors shown in Fig. 24 is the resonant tank for continuation of supply during rising and falling of the sine wave. It also continues to give supply during 2.5 % dead time of the switches in their state change. Voltage and frequency is controlled by pulse width modulation by changing duty ratio. Simulation graphs for PWM, load current and load voltage are shown and discussed in chapter V.

3.1.8.3 Control circuit

The flow chart Figure 2of *chapter 2* shows the power flow of the system in detail. The chart shows how the interface responds to the user selection. The system consists of an LCD display to indicate power level and switching frequency and also gives the system status for any user input. The program in the flow chart first asks the user to select desired power level. The selected power will send a specific signal to the system and the system will do a power analysis to check if the battery power is enough to supply the system. If the battery is not enough, the system will automatically switched into mains supply. After the cooking is done, the mains will than charge the battery.

The design consists of two power sources, i.e. solar and mains power. The two power sources are connected directly to the system. The mains power provides with +/- 230 V and that is converted into direct current via the converter since the system requires direct current input. The converted DC voltage is 48 V that is able to charger the battery storage and also be able to independently supply the system. The converter is connected with the first section of the battery charger control circuit for mains supply charging. The second section of the charging circuit is the MPPT regulator that is connected to the solar panel, if solar is selected to charge the battery instead of mains. This means that the battery storage can be charged either by solar or mains power but treating solar a priority power source. The MPPT is design to regulate the unregulated/ fluctuating DC voltage from the panel. Two panels of each 300 watts are used to provide a maximum of 600 watts. The user interface with the buttons is designed for the user to be able to select any power level required. Each power level is programmed with a specific switching frequency. The switching frequency is controlled by means of the duty ratio. Each complete circle of the pulse width modulation (PWM) is accommodated with a switching dead time of +/-5 % to allow the switches not to switch at the same time as this might result in a short circuit. The switching method used is zero voltage switching (ZVS), i.e. no voltage will be across the switches during the switching. The ZVS is achieved by switching at frequencies higher than the resonance frequency. The Fig. 23 below shows the overall simulation circuit of the design.

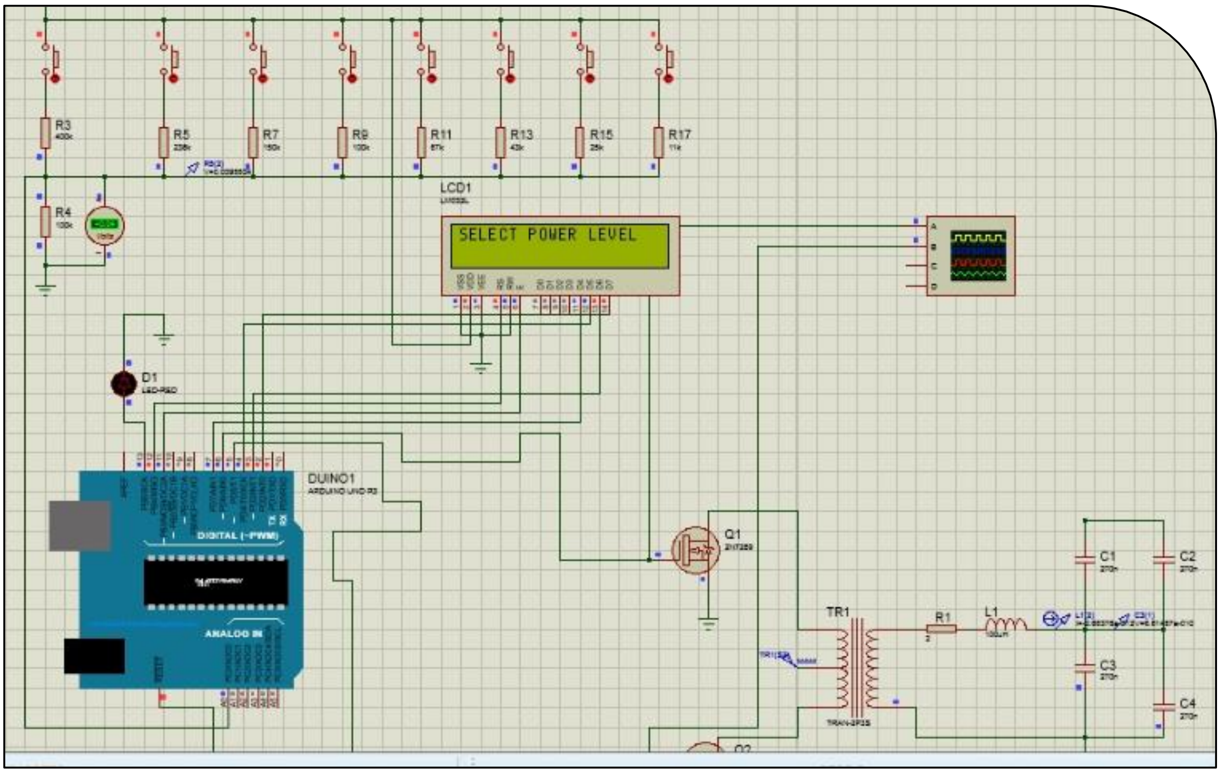

Figure 23: Whole circuit simulation diagram

3.2 Conclusion

At this stage, three chapters have been accomplished with success following the general and specific research objectives. *Chapter I* was more of a problem statement, including the benefits of solar applications in residential areas and the rationale for the proposed system for this study by looking at the advantages and disadvantages. The chapter went even deeper by looking in the general and specific objectives as to meet the design general and specific expected outcomes. Lastly it discusses about the contribution of the study in the research and also in the community with the brief arrangement of the thesis chapters at the end. *Chapter II* concentrates on the existing technologies relating to the study. The existing literature is studied and analysed accordingly by looking at the existing gaps and presenting the solutions amongst them. It also touches the design methodology by explain the circuit or design operation by means of flow diagram. Design stages are also explained in detailed outlining how the design is handled in terms of achieving general and specific objectives. From the two first chapters, the deep understanding of the research is achieved by means of generating general and specific objectives and also designs of the flow chart for power flow together with design stages. *Chapter III* is more of taking clear understanding of the research general and specific objectives from chapter I and II into practice by means of mathematical calculations and circuit analysis of all the design stages together with simulation diagrams. Some blocks in the block diagram are not simulated in terms making a circuit diagram like auto-switching. The auto-switching feature is explained by means of flow chart only and will be done using a programmable relay in *chapter IV* and also the MMPT regulator will be used to make things more easier for solar to the battery power flow. The following study is *chapter IV,* the chapter focuses on the design implementation of the system. And *chapter V* is the simulation and practical results obtained using the simulation diagrams in this chapter. It also gives the justifications for simulations and practical results for each block in the block diagram in section 3.1 of this chapter. *Chapter VI* is the thesis conclusion chapter.

4 Implementation Design

4.1 Introduction

The schematic below in Fig. 24 shows the actual design diagram for the design implementation. The system utilizes two power sources, namely; mains and solar as it can be seen below (as per design specification in Chap.1). The programmable relay is an auto-selection switching that is directly connected with the panel and on the normally open point (N/O) for the mains to allow auto switching if solar is removed or no enough solar radiation to make it operate. The MPPT block includes the DC-DC MPPT and AC-DC charger that allows the solar and mains to charge the batteries respectively. Solar is treated as a priority as per the design specifications discussed in the previous chapters. The battery bank utilizes the deep cycle batteries for it advantage of slow discharging and fast charging characteristics. Further analysis is give from section 4.1.1 – 4.1.5. The PCB layout and the circuit setup can be seen in appendix D.

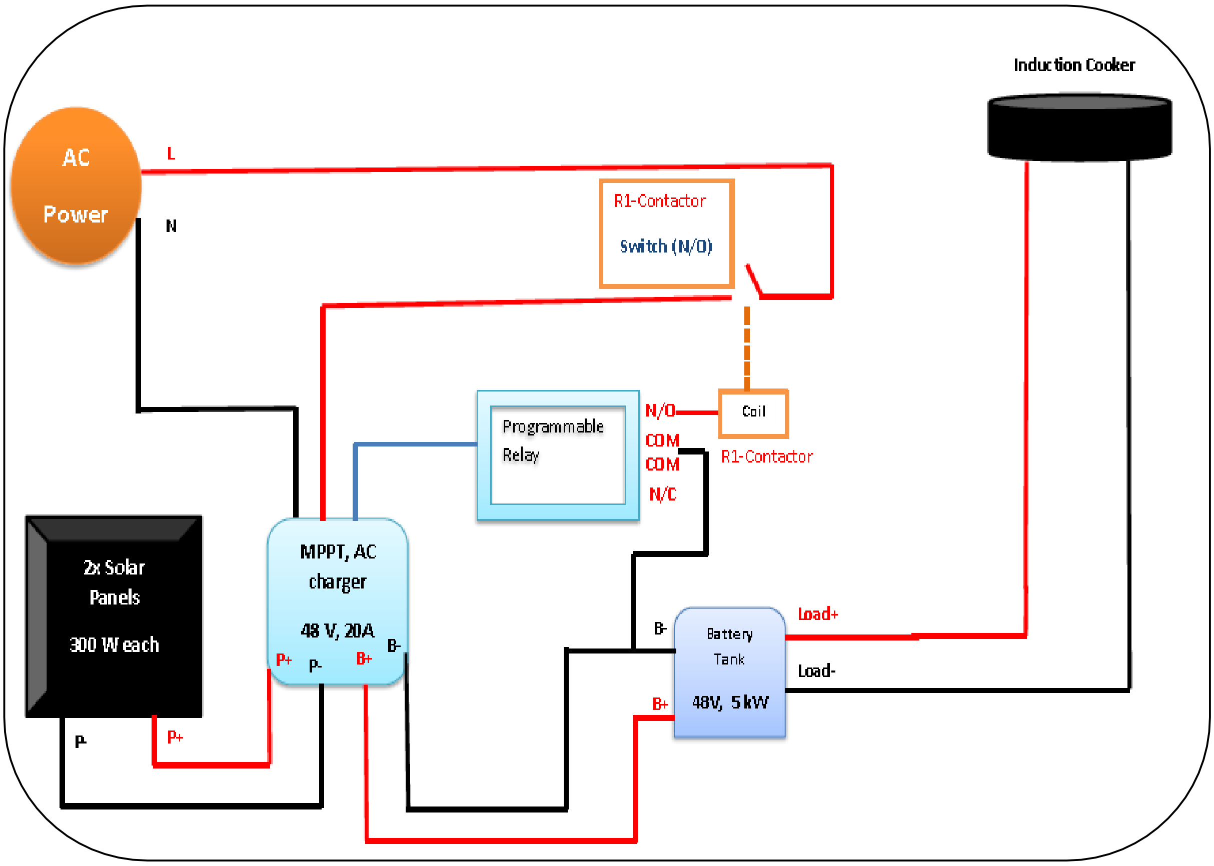

Figure 24: Implementation design schematic

4.1.1 Programmable relay, MPPT and AC-DC charger

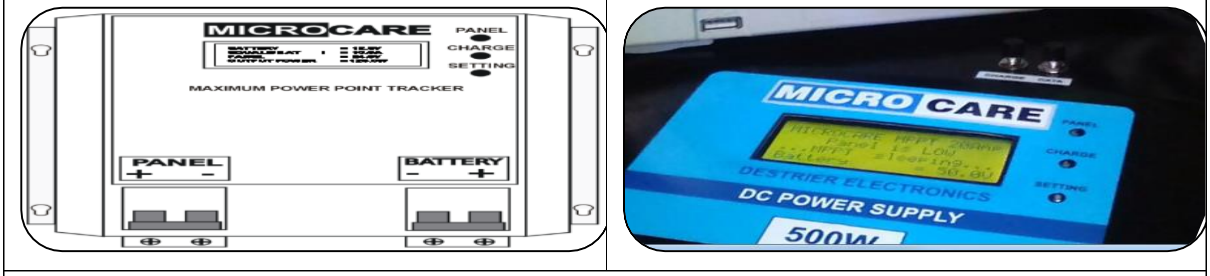

Figure 25: Microcare MPPT charger

The MPPT is used in the circuit implementation to easily program and use it for maximum power delivery from panel as seen in Fig. 25 above. The 20 *A* MPPT is used to allow it to be able to charger the four 105 *Ah* batteries used in the system. The unit is programed to detect battery low at 44 *V* to avoid draining batteries to low state as this can cause system low voltages and draw more current to compensate for the output voltage required at a specific power level and exposed the user to high currents at the output. The factor is that drawing batteries to it low voltage will shorten the life cycle of the batteries. The unit is integrated with the AC-DC charger and auto-switch relay to easily communicate as per the code running in the unit. The unit is designed at 500 watts maximum while the batteries form a 2 *kW* system and this means that the cooker can run at its maximum power for 4 hours without charging needed. The MPPT manual can be found on the MICROCARE website.

4.1.2 Battery storage

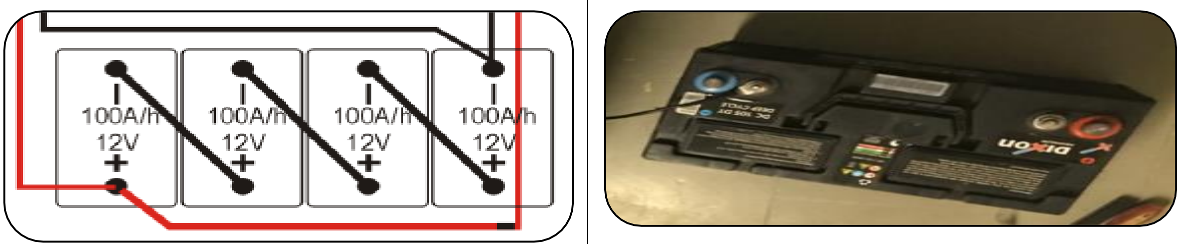

Figure 26: Battery wiring diagram

The system uses four times 105 *Ah*, 12 *V* Dixon deep cycles to make a 48 *V* system. The image above in Fig. 26 shows the actual battery used together with the wiring diagram on the left as the batteries are connected in series.

The batteries present high usage as their discharge gradient is very steep while the charging one is sharp curve. Safety precaution is followed as the batteries form a huge hazard for the user. The batteries need to be placed in a cool place, preferable less than room temperature. The batteries also require a recommended carrying during movement to keep the life cycle as the user out danger as it contains toxic fluids.

4.1.3 Induction cooker

The fig. 27 below shows the main components for the system design;

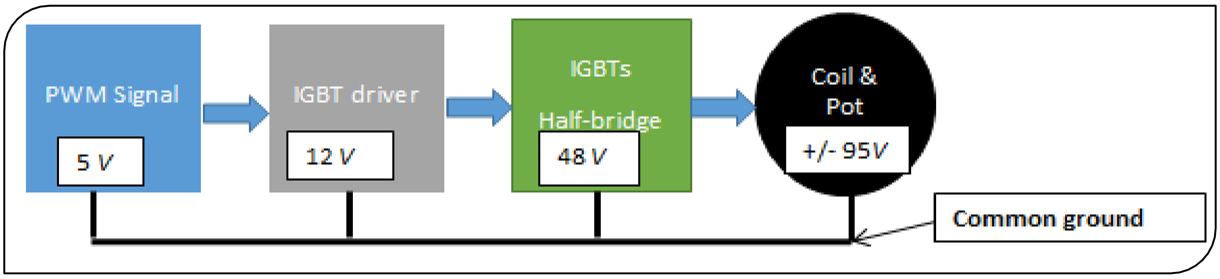

Figure 27: Cooker diagram

The microcontroller is programmed with eight power levels that are also displayed in the LCD as per the user selection (see appendix C, Fig. 48 for PCB circuit layout). The user selects any desired power level and a switching signal is generated at 5 *V*, get boosted by the IGBT driver to meet IGBT gate to collect switching voltage (12 *V*) and then supplied to the switches that is connected to 48 *V* DC bus voltages and convert it to AC to run the cooker. The results for all the switching power levels are show in the results section Figure (38-45) of chapter 5. Arduino microcontroller is the preferred choice due to it affordability, easy to program and having open source libraries that includes LCD. The common ground is shown to emphasize the importance that can affect the whole setup if not connected properly.

4.1.4 Driver circuit

The IGBT driver circuit plays a big role in the circuit operation. The drive acts as a voltage isolator between microcontroller and the DC bus voltage. It also boosts the input signal to a recognized switching voltage in the IGBTs. The circuit diagram can be seen on appendix (B) Figure 46. International rectifier driver is used (IR2184). The offset voltage is 600 *V* with fast turn off/on times that makes them to quickly distort the signal as soon as possible. It also presents short dead time that allows greater power transfer to the load. The driver uses 1 *uF* decoupling capacitor to reduce voltage spikes that might damage the circuit. The 100 *nF* is a bootstrap capacitor that act as a charge pump to switch the IGBTs.

4.1.5 Half bridge

The half bridge circuit consists of high and low side IGBT, inductor coil, pot and resonant capacitors. IGBTs were used instead of the MOSFETS due to its Ability to handle the high voltage (600V), low conduction and due to the frequency (10-65 kHz), IGBTs forms better option. This circuit utilizes the G4PC50F IGBT. This component was chosen due to its ultrafast switching, high input impedance, low conduction losses and low switching losses. The SGL160N60UFD IGBT is used in the circuit. The resonant capacitors are placed in parallel on either side of the load. Four 270nF used rather than two 540nF capacitors because high value capacitors have poor high frequency response properties and exhibit a high series parasitic resistance.

Figure 28: Half bridge inverter

The resistance Located in series between the driver signal and the IGBT gate in Fig. 28 above is a potentiometer. This acts as a gate resistor and limits the instantaneous current that is drawn when the IGBT is turned on it functions as a slew-rate limiting device for the gate signal, reduces ringing and voltage spikes. The IGBTs are mounted on a heat sink, which dissipates waster heat generated during switching into the surrounding air. An insulating pad and thermally conductive paste lie between the IGBTs and the heat sink. The insulating pad combines a film and silicone rubber and acts as a tough dielectric barrier against cut-through.

4.2 Circuit performance

CHAPTER IV

The induction cooker was implemented with success and is capable of generating enough heat. The Fig. 29 below shows the circuit performance during testing. The system uses one supply of 48 *V* DC to power all the circuits, 5 *V* for microcontroller and LCD, 12 *V* for IGBT drivers. All the input and output power parameters are displayed in chapter 5 (Table 5-17) together with each level output efficiency. The cooker was tested using water of about 700ml. The cooker managed to heat the water at approximately 100 °C from power level 5 upwards and this is due to the amount of power consumed by the load at the time. The water actually needs more energy to heat from 90 to 100 °C as more stronger bonds require sufficient energy to latent heat to convert liquid state to gas form.

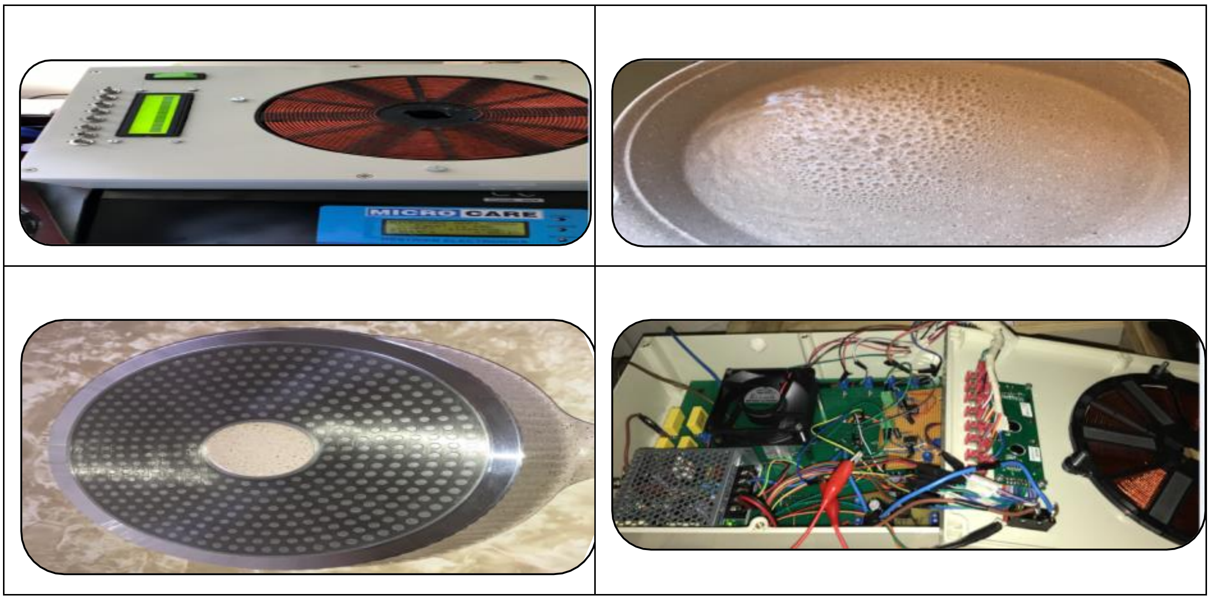

Figure 29: Induction cooker, pot, and whole setup

CHAPTER V

5 System Simulations and Practical results

5.1 Introduction

Induction cooker presents the most efficient way of cooking compared to the traditional cooking methods that are high in the market. The cooker also come with energy savings, cleanness and quicker in power delivering within seconds to reach maximum output as stipulated in chapter II and III. The solar powered cooker it even adds more on the power and money savings as explained in details in the previous chapters. The schematic and mathematical design in chapter III showed a proper circuit analysis together with necessary calculations to prove the feasibility of the solar powered induction cooker. The code can be seen in appendix (D) that runs in the background of the simulations and practical of the system. The code control the alternative switching of the two half-bridge IGBTs and work to display the power level and switching frequency. This chapter presents the simulation results gathered in the design and simulation circuits in chapter III. It also shows the corresponding practical results. Some of the circuits in the block diagram are not simulated but are shown in the practical results section to complete the design. Each simulation and practical result shows the pulse width modulation, load current and voltage. The output power is calculated using the load current and voltage. The current generated at the output is highly dependent on the pot material used during simulations and or practical. The simulations are shown and explained in section 5.2 followed by experimental results in section 5.3, results analysis in section 5.4, adjustments made to accommodate implementation of the design prototype together with proper justifications made from the simulations Section 5.5, circuit analysis in section 5.6 and future work in section 5.7. This chapter answers all the previous chapters by meeting general and specific objectives of the design and also answers the aim of the research. This is the core chapter of the study. The discussion at end of this chapter touches how this research meet the commercial product standards together with future research in the same study and how it can be improve from what has been done.

5.2 Simulation results

The simulation results for selection of various power levels are shown in Figures 30 to 37 together with power consumed in Table 5-1 to 5-8. The simulation design is tested using Proteus software. The results include pulse width modulation, current in the coil and the load voltage in the presence of the pot. The results differ with switching frequency. The frequency ranges from 10 kHz to 65 kHz. The simulations are carried out using one pot resistance value of 1.23 ohms as load. It is noted that changing the pot material can negatively or positively affect the output power keeping voltage and frequency constant. The higher the resistance the higher the output power and vice versa. The results shows simulations for all eight power levels as indicated in the design specific objectives in chapter I and II.

The Fig. 30 below shows power level one in a form of three waveforms, pulse width modulation frequency (PWM), load voltage and current respectively. The PWM switching signal is modelled in Proteus as mentioned above creating a pulse voltage of 5 *V* to drive the two half bridge IGBTs alternatively to allow it not to switch at the same time. 5 *V* is only able to drive the switches in the simulation as the IGBTs are ideally and no need of the driver circuit to amplify the signal. The two PWM signals yellow (high-side) and blue (low-side) has a dead time of about 5 – 10 % per cycle to allow smooth switching. It can be noted that there is a small distortion in the PWM but with no measure effects in the driving of the inverter circuit. The noted distortion can result in a temperature rise in the IGBTs. This will be dealt with correct with the use of the isolators and trimmers to make it smooth in the implementation section 4. The voltage and current are almost sinusoidal with a peak voltage of 60 *V* and peak current of 6 *A*. Fig. 30 is further followed by Table 5-1 that represent the RMS values of the source and load currents and voltages to get the actually power supplied and consumed at power level one. The efficiency of the system is behaving ideally as expected due that no real components with different tolerances to contribute to external losses. Thus the results in the Fig. 30 and Table 5-1 are expected to differ in the practical stage. All the other following power levels from Fig. 31 – 37 have a similar trend to the current Figure but differ slightly and all the differences will be mentioned in all the Figures.

PWM Level one 62.5 *kHz*

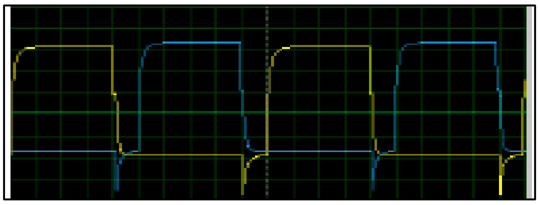

Load voltage 60 *V*

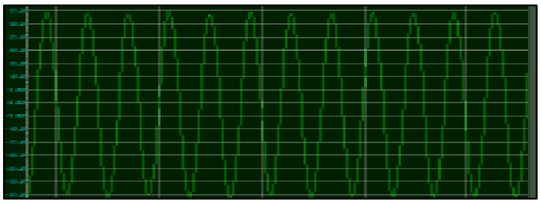

Load current 6 *A*

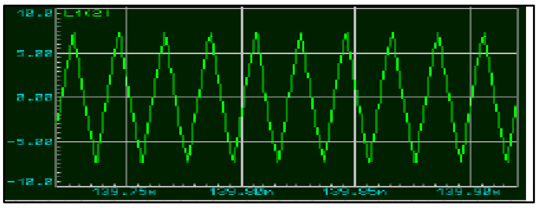

Figure 30: Power level one

Table 5 -1: power level one result

Inputs		**Outputs**	
V_{RMS}	48 *V*	V_{RMS}	42.43 *V*
I_{RMS}	3.98 *A*	I_{RMS}	4.24 *A*
P_{IN}	191.04 *W*	P_{OUT}	180 *W*

The power two is displayed in Fig. 31 in the same order as from Fig. 30 above. The difference from the Fig. 30 is the switching frequency (50 kHz) that result in the increased in duty ratio and thus increases the ON time of the IGBTs to allow more power delivery to create larger output. It can be noted that the load voltage is still the same but current did increase and the waveform is no longer semi-sinusoidal. The increased in current is caused by a longer on time of the IGBTs that results in more magnetic field line passing through the pot resistance. There is a slightly difference in the load current peak value and the power consumed can be seen in Table 5-2.

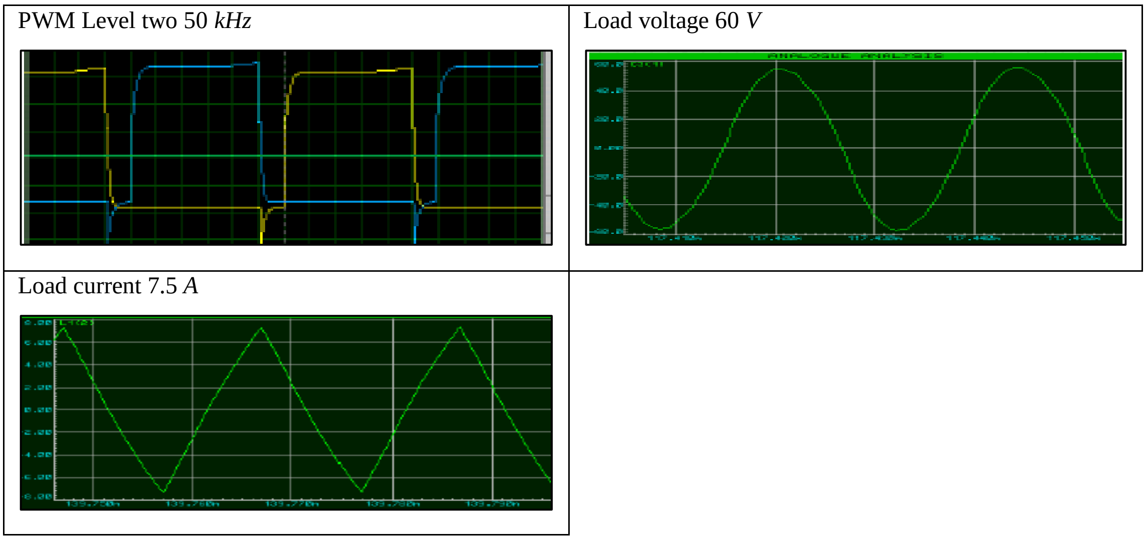

Figure 31: Power level two

Table 5 -2: power level two results

Inputs		Outputs	
V_{RMS}	48 *V*	V_{RMS}	42.43 *V*
I_{RMS}	4.80 *A*	I_{RMS}	5.30 *A*
P_{IN}	230.4 *W*	P_{OUT}	225.01 *W*

Power level three is shown in the Fig. 32 below. The PWW (41.67 kHz) signal is starting to get more distorted as the frequency increases and this is due to the increased in the load current that interact with the switching signal via the collector and the emitter. This will be minimized or sorted by the isolator (snubber circuit). The larger the load current, the larger the dead time for smooth switching. The load voltage is still the same and only current is changing and this is due to the similarity explained above.

PWM Level three 41.67 *kHz* 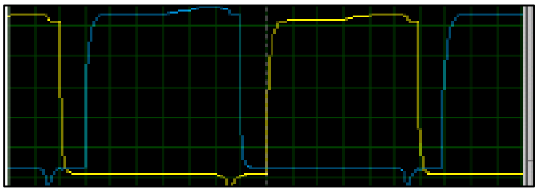	Load voltage 60 *V* 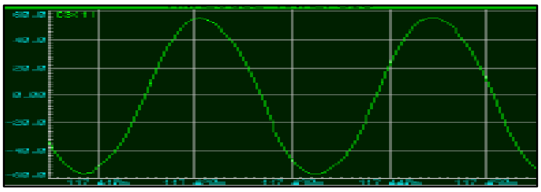
Load current 12 *A* 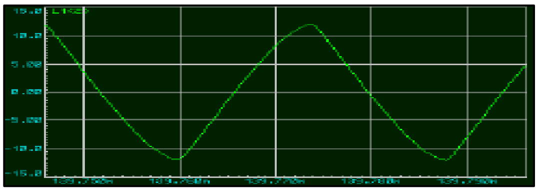	

Figure 32: Power level three

Table 5 --3: Power level three results

Inputs		**Outputs**	
V_{RMS}	48 *V*	V_{RMS}	42.43 *V*
I_{RMS}	7.80 *A*	I_{RMS}	8.48 *A*
P_{IN}	374.40 *W*	P_{OUT}	360.03 *W*

Power level 4-6, Fig. 33-35 have a similar trend of increased in switching frequency, same load voltage and more similar load current waveform but increasing in peak to peak value. This is due to that these frequencies are now closer to resonance frequency as seen in Fig. 18 of chapter 3. It can be seen from the mentioned figures how the distortion changes and how the load current is changing as well. All the analysis is done using one pot resistance.

PWM Level four 35.71 *kHz* 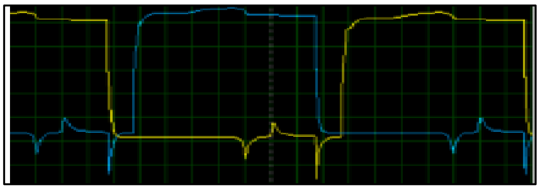	Load voltage 60 *V* 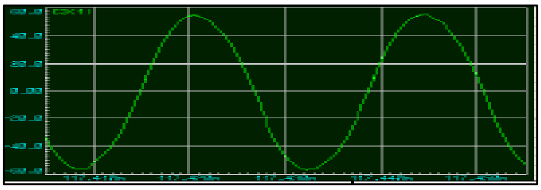
Load current 13 *A* 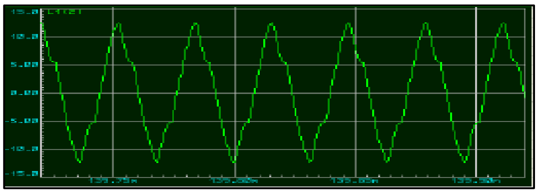	

Figure 33: Power level four

Table 5 --4: Power level four results

Inputs		**Outputs**	
V_{RMS}	48 *V*	V_{RMS}	42.43 *V*
I_{RMS}	8.30 *A*	I_{RMS}	9.19 *A*
P_{IN}	398.40 *W*	P_{OUT}	390.03 *W*

PWM Level five 27.78 *kHz* 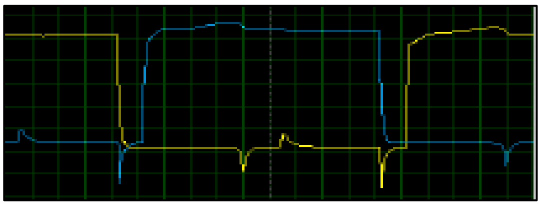	Load voltage 60 *V* 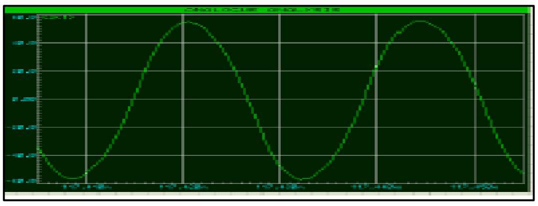
Load current 15 *A* 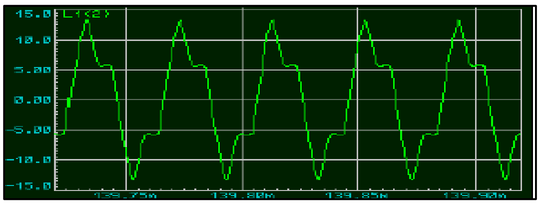	

Figure 34: Power level five

Table 5 -5: Power level five results

Inputs		**Outputs**	
V_{RMS}	48 *V*	V_{RMS}	42.43 *V*
I_{RMS}	9.50 *A*	I_{RMS}	10.60 *A*
P_{IN}	456.0 *W*	P_{OUT}	450.03 *W*

It is noted that power level 6 (Fig. 35) is the same as power level due to that their frequency lie in side and thus contribute to the same power level.

PWM Level six 20 *kHz*

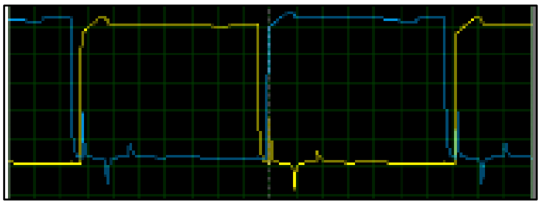

Load voltage 60 *V*

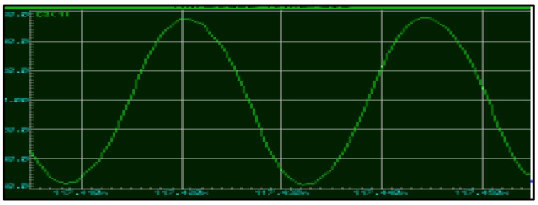

Load current 13 *A*

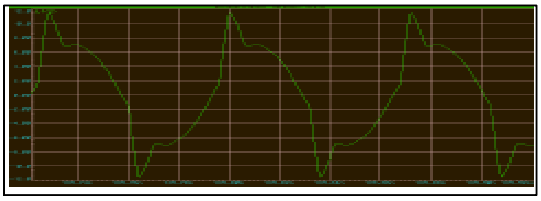

Figure 35: Power level six

Table 5 -6: Power level six results

Inputs		**Outputs**	
V_{RMS}	48 *V*	V_{RMS}	42.43 *V*
I_{RMS}	8.30*A*	I_{RMS}	9.19 *A*
P_{IN}	398.4 *W*	P_{OUT}	390.03 *W*

Fig. 36 shows the second to last power level at 15.15 kHz. The duty ratio can be noticed increasing even further at this switching stage. The dead time is a bit small and high power is produced at this stage. This switching signal lies almost around the resonance. The load voltage is also increased slightly and that is caused by the change inductance as the approaching resonance. The RMS values are stipulated in Table 5-7.

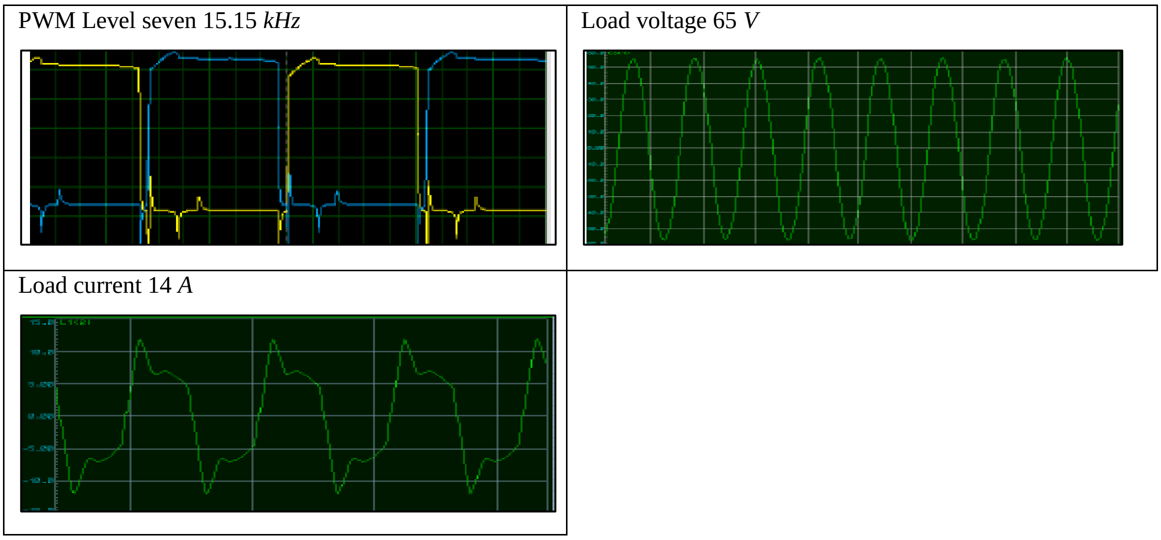

Figure 36: Power level seven

Table 5 -7: Power level seven results

Inputs		**Outputs**	
V_{RMS}	48.0 *V*	V_{RMS}	45.96 *V*
I_{RMS}	9.60 *A*	I_{RMS}	9.89 *A*
P_{IN}	460.80 *W*	P_{OUT}	454.98 *W*

Power level 8 below in Fig. 37, shows a very high voltage shoot as results of resonance. Equation (10) in chapter III shows a great relationship between inductance and capacitance. At resonance, capacitive and inductive reactance's re approximately the same and thus can expect a huge rise and RMS voltage as a result. Load voltage is peaking at 180 *V*. For the induction cooker, it is not expected to have such big power consumed by the load. This is happening just because the simulations source is not limited in terms of how much the load is expected to draw. The maximum power is expected to be around 500 watts for the cooker as almost more than 80 % of the power is converted to cooking and thus require less power.

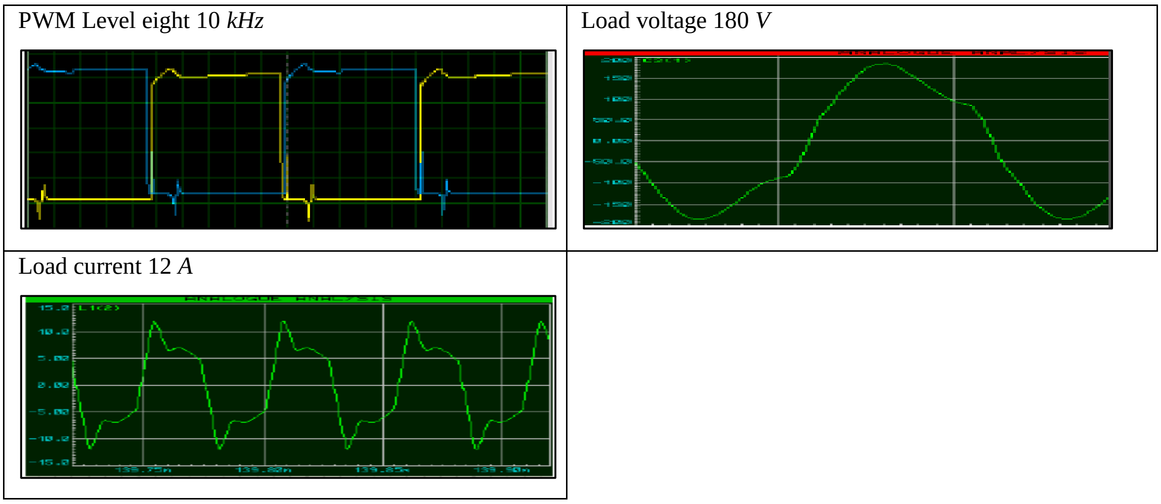

Figure 37: Power level eight

Table 5 -8: Power level eight results

Inputs		**Outputs**	
V_{RMS}	48 *V*	V_{RMS}	127.28 *V*
I_{RMS}	22.80 *A*	I_{RMS}	8.49 *A*
P_{IN}	1094.40 *W*	P_{OUT}	1080 *W*

5.3 Experimental results

The practical results are shown below from Fig. 38-45 together with the power that is consumed in Table 5-9 to 5-16 during operation. The results shows the PWM with different switching frequency, which goes with load current and voltage to show power that is consumed by the load during operation. The results were taken in Durban at Tower residence the University of Kwa-Zulu Natal.

Figure 38 shows the practical results of power level one for the induction cooker testing. The testing was performed using oscilloscope to capture all the readings. The signals were taking using a smart phone device. This figure below was expected to give same results as of Fig. 30 in the simulation results. The first challenge was that, the simulations were using an unlimited source that was not controlled in terms of how much the circuit is going to draw at a specific frequency. Frequency was the only controlled variable during the simulations and practical. It is not possible to use an unlimited source in the practical section as this can course burning issues in the circuit and as for safety of the user, testing purposes; the 500 watts power supply was used. The waveform signals are similar, though the actual peak values differ as adjustments were made in terms limited component usage. The Table 5-9 gives the RMS values for input and output parameters to calculate power consumed, together with its efficiency as indicated in Table 5-17 at the end of this chapter.

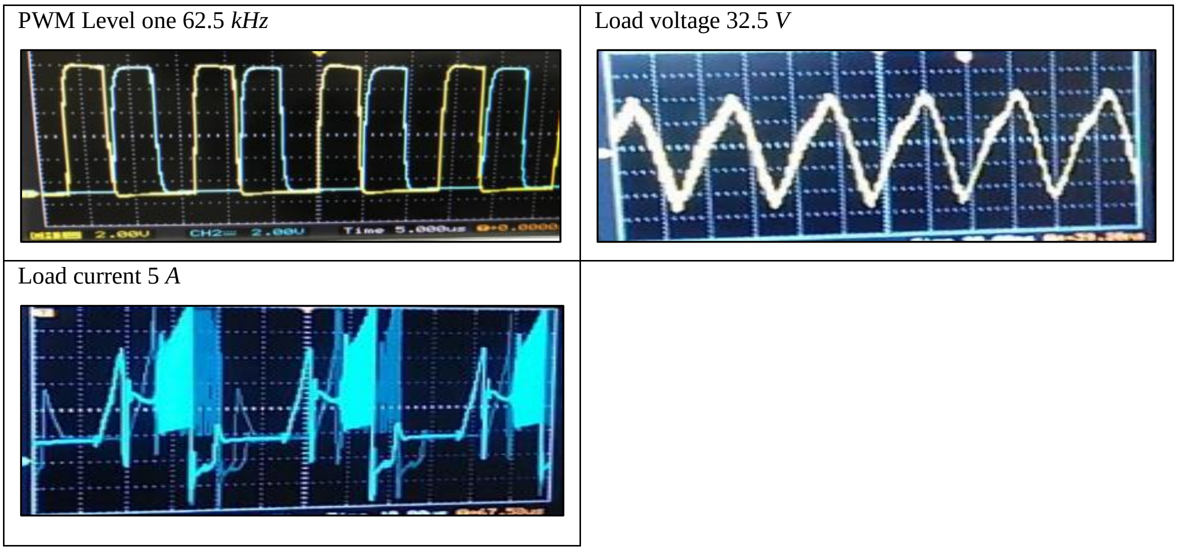

Figure 38: Power level 1

Table 5 -9: Power level one result

Input (s)		Output (s)	
V_{RMS}	49.9 *V*	V_{RMS}	22.98 *V*
I_{RMS}	2.40 *A*	I_{RMS}	3.54 *A*
P_{IN}	119.76 *W*	P_{OUT}	81.25 *W*

From Fig.39, it can be noted that in the practical section, the current remains the same for power level 1 and 2 and only the load voltage that is changing. This is due to the resonant capacitors used in the practical which can take more current spikes from the induction coil and give a smooth larger voltage instead of high current for such low power stages. It can also be seen the load voltage signal is a bit distorted, which is caused by the increased in voltage.

PWM Level two 50 *kHz*

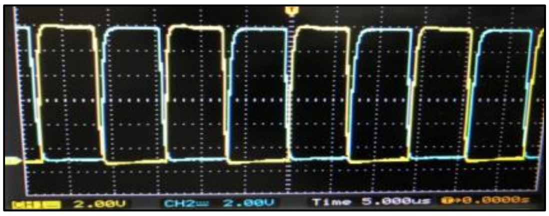

Load voltage 50.12 *V*

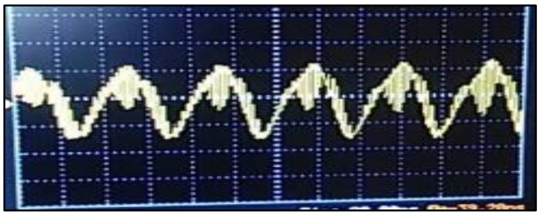

Load current 5 *A*

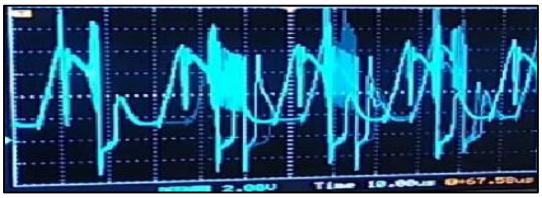

Figure 39: Power level two

Table 5 -10: Power level two results

Input (s)		Output (s)	
V_{RMS}	48.90 *V*	V_{RMS}	35.44 *V*
I_{RMS}	3.2 *A*	I_{RMS}	3.54 *A*
P_{IN}	166.26 *W*	P_{OUT}	125.30 *W*

Figure 40 shows the practical results for power level 3. The value of the load current is still constant as for the reason explained above. The load voltage and switching frequency are the only parameters changing. The Table 5-11 gives the actual RMS values and power consumed by the load at the time. The dead time was programmed per each power level as to meet correct switching characteristics.

PWM Level three 41.67 *kHz*	Load voltage 67.4 *V*
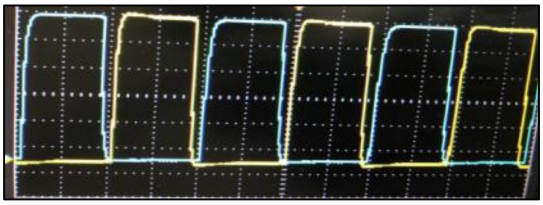	
Load current 5.2 *A*	
	

Figure 40: Power level three

Table 5 -11: Power level three results

Input (s)		Output (s)	
V_{RMS}	48.8 *V*	V_{RMS}	47.66 *V*
I_{RMS}	4.60 *A*	I_{RMS}	3.68 *A*
P_{IN}	224.48 *W*	P_{OUT}	175.24 *W*

Fig. 41-42 have the same load voltage but different load currents. This is due to that the switching frequencies for the two power levels which lie in same point in the frequency power curve in Fig. 18 (chapter 3) but the ON time duty ratio is not the same and thus output power is different.

PWM Level four 35.71 *kHz*

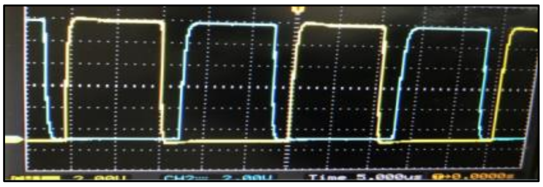

Load voltage 78.2 *V*

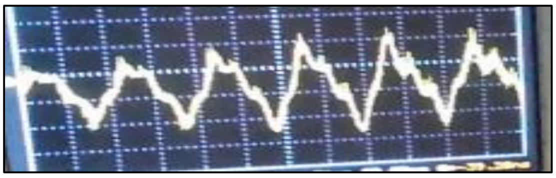

Load current 5.5 *A*

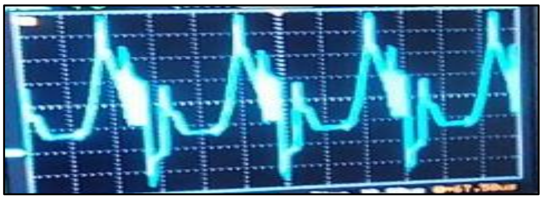

Figure 41: Power level four results

Table 5 -12: Power level four results

Input (s)		Output (s)	
V_{RMS}	48.60 *V*	V_{RMS}	55.15 *V*
I_{RMS}	5.40 *A*	I_{RMS}	3.90 *A*
P_{IN}	262.44*W*	P_{OUT}	215.09 *W*

PWM Level five 27.78 *kHz*

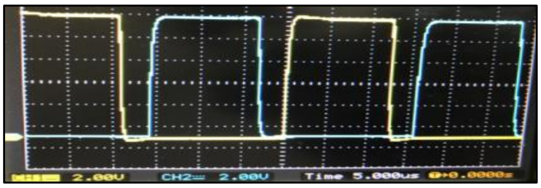

Load voltage 78.2 *V*

Load current 7.3 *A*

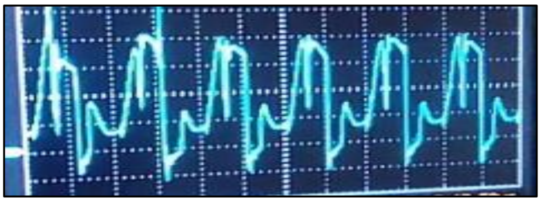

Figure 42: Power level five

Table 5 -13: Power level five results

Input (s)		Output (s)	
V_{RMS}	48.50 *V*	V_{RMS}	55.15 *V*
I_{RMS}	6.70 *A*	I_{RMS}	5.16 *A*
P_{IN}	324.95 *W*	P_{OUT}	284.68 *W*

It is noted that Fig. 43-45 have the same load voltage but differ in load currents. This is due to more magnetic field line entering the pot at a time and results in a rise in the load current in the pot. Remember, current generated at the load depends directly on the load resistance and switching frequency. It is also noted that efficiency increases with the increase in power levels as fast switching is adapted. Table 5-14 to 5-16 shows the actual RMS values of the input and output parameters.

PWM Level six 20 *kHz*

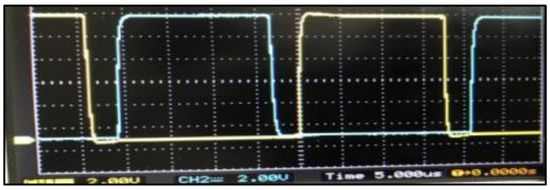

Load voltage 94.4 *V*

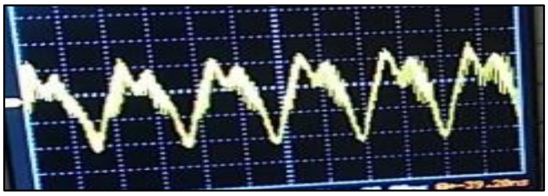

Load current 6.5 *A*

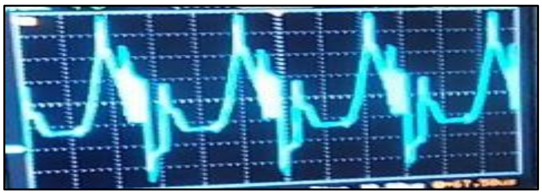

Figure 43: Power level six

Table 5 -14: Power level six results

Input (s)		Output (s)	
V_{RMS}	48.30 *V*	V_{RMS}	66.75 *V*
I_{RMS}	7.1 *A*	I_{RMS}	4.60 *A*
P_{IN}	342.93 *W*	P_{OUT}	306.80 *W*

PWM Level seven 15.15 *kHz*

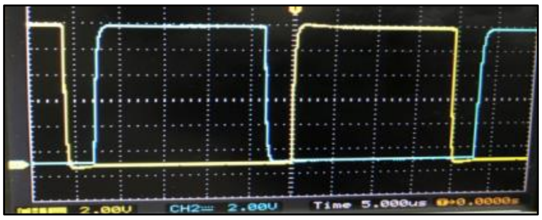

Load voltage 94.6 *V*

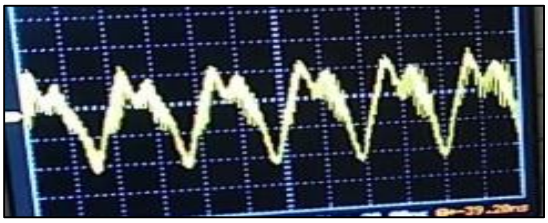

Load current 7.5 *A*

Figure 44: Power level seven

Table 5 -15: Power level seven results

Input (s)		Output (s)	
V_{RMS}	48.10 *V*	V_{RMS}	66.75 *V*
I_{RMS}	8.2 *A*	I_{RMS}	5.30 *A*
P_{IN}	394.42 *W*	P_{OUT}	353.99 *W*

PWM Level eight 10 *kHz*

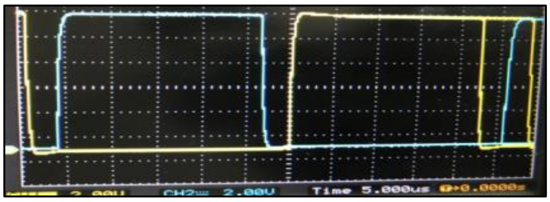

Load voltage 94.9 *V*

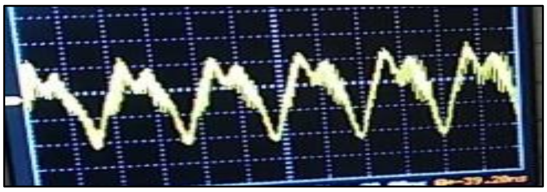

Load current 9.1 A

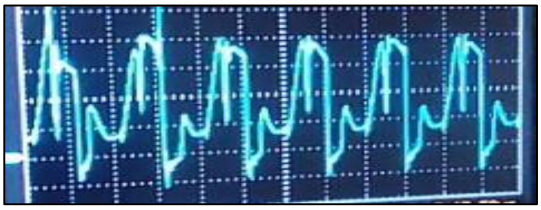

Figure 45: Power level eight

Table 5 -16: Power level eight results

Input (s)		Output (s)	
V_{RMS}	48.05 V	V_{RMS}	66.75 V
I_{RMS}	9.8 A	I_{RMS}	6.44 A
P_{IN}	470.40 W	P_{OUT}	429.51 W

5.4 Results Analysis and Discussion

5.4.1 Simulations vs. Practical

The Table 5-17 below shows the input and output parameters for both simulations and practical results. The peak values from Fig. 38-45 are converted to root mean square to get the actual current and voltage in order to get power and efficiency for each power level. It can be noted that as the frequency decreases (from low power); the power output is increased simultaneously and vice versa. The table below indicates cooker switching power levels from low to high power level respectively. It can be seen that the efficiency increases with increased in switching frequency and that means lower power frequencies are less efficient than the ones closer to resonant. Low efficiency in power level 1-3 is caused by the huge losses in the IGBT as the switching is a bit slower compared to the rest of the power levels. There is a study of dual-mode in induction heating that discusses about the induction heater with two half-bridge inverters. It is classified as class D and DE for high and low power output range respectively. The combination of the two operating modes of the classes achieves high efficiency for a wide range of power output [31].

5.4.2 Circuit Performance

5.4.2.1 Efficiency

The implemented system is a 500 watts supply. All the power dissipation of the important components was measured using 500 watts operating power. The losses can be of IGBT, diode, filter and coil. These losses are estimate that the cooker efficient is expected to be around 80 %. The efficiency of the cooker is tested to determine its performance. Equation (17) below is used to determine efficiency of the system using input and output parameters as seen in the table 5-17 below.

$$\zeta = \left(1 - \left(\frac{P_{in} - P_{out}}{P_{in}}\right)\right) \times 100 \qquad (17)$$

Table 5-1 shows the circuit characteristics of the system of the cooker from power level 1-8 respectively. The switching frequency ranges from 62.5- 10 kHz. It can be seen that the simulation system efficiencies ranges above

90 % while the practical starting at about 67 % up to 91 %. This is caused by the low switching signals that result in too many losses in the IGBTs. These power levels from 1-3 as seen in the figure below are probably the one used in commercial induction cooking applications as great system settings that can be used for a longer period. But those efficiencies can be improved further with the application of dual mode discussed earlier. Power level 4-8 efficiencies ranges from 80 - 90 %. These are very encouraging and it is due to the following reasons; using only half-bridge (2 IGBTs), safe dead time, running the cooker close to resonance frequency. The sharp drop in efficiency is caused by the system losses explained in paragraph 1 of this section.

Table 5 -17: Simulations and practical results overview

Simulation results				**Practical results**			
Input (s)		**Output (s)**		**Input (s)**		**Output (s)**	
V_{in}	48 *V*	V_{out}	42.43 *V*	V_{in}	49.9 *V*	V_{out}	42.43 *V*
I_{in}	3.98 *A*	I_{out}	4.24 *A*	I_{in}	2.40 *A*	I_{out}	4.24 *A*
P_{in}	191.04 *W*	P_{out}	180 *W*	P_{in}	119.76 *W*	P_{out}	180 *W*
		ξ	94.22 %			ξ	67.84 %
Power level one							
V_{in}	48 *V*	V_{out}	42.43 *V*	V_{in}	48.90 *V*	V_{out}	35.44 *V*
I_{in}	4.80 *A*	I_{out}	5.30 *A*	I_{in}	3.2 *A*	I_{out}	3.54 *A*
P_{in}	230.4 *W*	P_{out}	225.01 *W*	P_{in}	166.26 *W*	P_{out}	125.30 *W*
		ξ	97.66 %			ξ	75.36 %
Power level two							
V_{in}	48 *V*	V_{out}	42.43 *V*	V_{in}	48.8 *V*	V_{out}	47.66 *V*
I_{in}	7.80 *A*	I_{out}	8.48 *A*	I_{in}	4.60 *A*	I_{out}	3.68 *A*
P_{in}	374.40 *W*	P_{out}	360.03 *W*	P_{in}	224.48 *W*	P_{out}	175.24 *W*
		ξ	96.16 %			ξ	78.06 %
Power level three							
V_{in}	48 *V*	V_{out}	42.43 *V*	V_{in}	48.60 *V*	V_{out}	55.15 *V*
I_{in}	8.30 *A*	I_{out}	9.19 *A*	I_{in}	5.40 *A*	I_{out}	3.90 *A*
P_{in}	398.40 *W*	P_{out}	390.03 *W*	P_{in}	262.44 *W*	P_{out}	215.09 *W*
		ξ	97.98 %			ξ	81.95 %
Power level four							
V_{in}	48 *V*	V_{out}	42.43 *V*	V_{in}	48.50 *V*	V_{out}	55.15 *V*

I_{in}	9.50 *A*	I_{out}	10.60 *A*	I_{in}	6.70 *A*	I_{out}	5.16 *A*
P_{in}	456.0 *W*	P_{out}	450.03 *W*	P_{in}	324.95 *W*	P_{out}	284.68 *W*
		ξ	98.68 %			ξ	87.60 %
Power level five							
V_{in}	48 *V*	V_{out}	42.43 *V*	V_{in}	48.30 *V*	V_{out}	66.75 *V*
I_{in}	8.30*A*	I_{out}	9.19 *A*	I_{in}	7.1 *A*	I_{out}	4.60 *A*
P_{in}	398.4 *W*	P_{out}	390.03 *W*	P_{in}	342.93 *W*	P_{out}	306.80 *W*
		ξ	97.98 %			ξ	89.70 %
Power level six							
V_{in}	48.0 *V*	V_{out}	45.96 *V*	V_{in}	48.10 *V*	V_{out}	66.75 *V*
I_{in}	9.60 *A*	I_{out}	9.89 *A*	I_{in}	8.2 *A*	I_{out}	5.30 *A*
P_{in}	460.80 *W*	P_{out}	454.98 *W*	P_{in}	394.42 *W*	P_{out}	353.99 *W*
		ξ	98.69 %			ξ	89.75 %
Power level seven							
V_{in}	48 *V*	V_{out}	127.28 *V*	V_{in}	48.05 *V*	V_{out}	66.75 *V*
I_{in}	22.80 *A*	I_{out}	8.49 *A*	I_{in}	9.8 *A*	I_{out}	6.44 *A*
P_{in}	1094.40 *W*	P_{out}	1080 *W*	P_{in}	470.40 *W*	P_{out}	429.51 *W*
		ξ	98.72 %			ξ	91.30 %
Power level eight							

5.5 Simulation and Practical results comparison and justification

Section 5.2 to 5.3 shows the results for the simulations and practical respectively. For the practical, 1.01 Ω pots was used for demonstration and that affect the results as power generated in the load depends on the coupling pot with the inductor. There are some changes that where adapted in order to meet practical circuit implementation and testing. See appendix C for simulation, practical results together with system efficiency for each power level. Below is the list of changes made to accommodate design implementation;

- 105 *Ah* batteries used instead of the 25 *Ah* proposed to accommodate system stability.
- IGBT driver circuit used to meet IGBT collector to emitter switching voltage.
- The pot resistance use in the theoretical calculations is slight bigger than the one use in the practical and that brings large power difference.
- The power supply is designed at 500 watts maximum and it can only produce up to maximum as this is a prototype to demonstrate the working principle of the idea. To also reduce chances of being exposed to high current that might result in injuries during building and testing.

- The mains AC to DC converter / charger is no longer connected direct to the cooker but both the solar and the mains are to charge the battery bank to completely make the cooker a standalone product that only work with the batteries.
- A lot of assumptions were made to meet the design general and specific objective.

5.6 Circuit results analysis

The aim of this section is to analyse the system operating characteristics. The analysis covers the evaluation of the achievements from solar panel, mains, MPPT up to inverter and induction cooker and the system strength and weaknesses.

5.6.1 Achievement

- The design and the manufacture of the AC to DC 48 *V* charger went very well as per the design specifications in chapter 1.
- The design and the programming of the MPPT regulator were tested and work successfully.
- The integration of the mains and the solar via programmable relay with as per the general and specific requirements.
- The automatic switching went well as well and demonstrated the feature of auto-switching and taking solar as a priority.
- The battery storage is charging perfect in both the power sources.
- The main part of design, the cooker performed absolutely fantastic of which is way better than was expected.
- All the design specifications in general and specific objectives were met, though maximum design power output for the prototype was different from what was used in the simulations.

5.6.2 Strengths

- The cooker successfully heated the pot using the principle of electromagnetic induction by varying switching frequency.
- The components to construct the cooker are very few, cheap and affordable.
- The efficiency is very encouraging from power level three upwards and this will prolong the life cycle of the components used and decrease cooling requirements and expenses.
- Battery tank can run the cooker at it maximum for about 6 hours with charging needed.

- The cooker output power levels and its efficiency is comparable and can compete with the commercial cookers in the market. This analysis was tested and proven by comparing the electric stove, commercial cooker and this cooker I have designed with the advantage of being flexible in terms of power sources.
- The system can also run the whole house lighting, charge cell phones, play radio and television at the same time if proper inverter is connected in the system.

5.6.3 Weakness

- The switching PWM from the microcontroller must be applied first to the IGBT gates before the 48 *V* can be switched on due to frequency bouncing and that can damage the IGBT straight away by shorting the emitter and the collector.
- The second drawback comes with low efficiencies at low power levels which fail to heat water up to its boiling point.
- High power levels cannot run for too long, like more than 30 minutes as IGBTs get hot and damaged after some time. This can be fixed by getting good PWM signal trimmers to minimize spikes in the switching signal.
- The confident shows that the minor drawbacks can be sorted provide that necessary alterations are done to 100 % meet the general and specific objectives.

CHAPTER VI

6.1 Conclusion

The induction cookers in the market use mains power to operate of which limits the flexibility in terms of power sources. The working principle of the project is similar to what is in the literature, but with more of advancement features using auto selection in terms power sources, taking solar as a priority with the addition of battery storage as a backup and also to make it a complete portable standalone product. The benefits includes, economic of which the energy is free from sun, environmental looks at zero released of toxic gases in the atmosphere and health in terms decreasing the amount of fossil fuels usage. The cookers in the market are completely dependent into electricity generated by Eskom. The introduction of solar energy comes with the aim of filling the big gap existing amongst the use of electricity that is 100 % dependent on non-renewable resources. It is also working in line with the sustainable development plan from department of energy. 98 % of the literature study proves that almost all the stoves in the market from electric, gas and induction cookers depends on non-renewables resources to operate. There is only one paper discussing about solar induction cooker but lacking a lot of advancement as it is a very low power, low efficiency and not flexible in terms of power sources as the country still run with non-renewables. This makes the paper to not compete with the cookers in the market. The general and specific objection of the smart solar powered induction cooker were met though they were some slightly adjustments made to accommodate the implementation as explain in chapter 4. All the design stages explained in chapter 2 were followed and met. The arrangement of the thesis is done in the form of chapters 1-6 of which are classified in specific topics given per chapter. This research was done following proper scientific processes including all the aspects including studying the design and following the right methods as form of presenting quality of research. The design is proven to meet the commercial standards as explained in chapter 4 of which brings a very big completion. The only factor to note is that installing the product is expensive (see Appendix C, Table C-1 and 2) though the costs can be recovered in about 4-5 years' time and make massive saving. The system can manage to run the whole house appliance of a small family home and can be adjusted accordingly to meet user requirements as per the appliances in the house. It is proven as from (Appendix C, Table C-3) using the power estimation that running a 2 plates electric stove with a consumption of 1.5 kW can take about 8 kW in 4 hours' time, while the induction cooker can run at one third of 1.5 kW and still produce efficient results taking only 2 kW in 4 hours. The system is proven to provide savings at about more 50 % for cooking purposes and about 70 % if all the appliances like television, radio, lights, charging cell phone and etc. can be integrated with the system.

6.2 Future work

There is a number of modifications that can be done in the project in order for it to be further developed as per below;

- Design a circuit to trim the voltage spikes in the PWM signals to reduce IGBT from heating.
- Use a bigger microcontroller with more pins like atmega32 to have enough pins for all the circuit programing as reset button is used to clear the signal after every switching done.
- Design and add a dual mode half bridge to improve the efficiency of the circuit as discussed in chapter 4.
- The other feature can be to design a pot detection circuit as the circuit cannot work without the pot being present.
- The system is capable of running cooker, house lighting, and television, charging cellphones (Put inverter) and running other small power consuming devises. This can bring lots of benefits for the user in decreasing the electricity bills even more.

References

[1]S. Villacís, J. Martínez, A. Riofrío, D. Carrión, M. Orozco and D. Vaca, "Energy Efficiency Analysis of Different Materials for Cookware Commonly Used in Induction Cookers", *Energy Procedia*, vol. 75, pp. 925-930, 2015.

[2] J. Acero et al., "The Domestic Induction Heating Appliance: An Overview of Recent Research," *In Proc. Appl. Power Electron. Conf Expo*, 2008.

[3] Carlos Sagues Blazquiz and Gonzalo Lopez-Nicolas, "Reset observers and temperature control for induction hobs," Universidad de Zaragoza, Spain, Zaragoza, Phd Thesis 2254-7606, 2011.

[4] D. C. Jiles and D. L. Atherton, "Theory of ferromagnetic hysteresis," *Journal of Magnetism and Magnetic Materials*, 1986.

[5] Sadhu, Pradip Kumar, et al. "A Comparative Survey on High Efficient Clean Heat Production through Microwave Oven and Induction Cooker."

[6] C.Ekkaravarodome, P. Charoenwiagnuea, K. Jirasereeamornkul, "The Simple Temperature Control for Induction Cooker based on Class-E Resonant Inverter", 2013 IEEE 10th conference on Electrical Engineering, Electronics, Computer, Telecommunications and Information Technology (ECTI-CON), pp 1-6, May 2013.

[7] ENERGY, ON RENEWABLE. "WHITE PAPER ON RENEWABLE ENERGY." (2003).

[8] Asmarashid Ponniran , Abdul Fatah Mat Said "DC-DC Boost Converter Design for Solar Electric System" International Conference on Instrumentation, Control & Automation ICA2009, ISBN 978-979-8861-05-5 pp-210-214.

[9] Cerri, Graziano, et al. "Rigorous electromagnetic analysis of domestic induction heating appliances." *PIERS Online* 5.5 (2009): 491-495.

[10] Lucia, Oscar, et al. "Efficiency-oriented design of ZVS half-bridge series resonant inverter with variable frequency duty cycle control." *IEEE Transactions on Power Electronics* 25.7 (2010): 1671-1674.

[11] Bhavana Ffion, Faseen.K., and Hema Mohan, "Solar Based Induction Cook Top", 3rd Int. Conf. on Electronics, Biomedical Engineering and its Applications (ICEBEA'2013) April 29-30, 2013, Singapore.

[12] Chun-Liang, H., 2007, July. Circuits analysis of inductive heating-device with half-bridge resonated inverter. In *11th WSEAS Int. Conf. Circuits* (pp. 26-30).

[13] Sweeney, Micah, et al. "Induction Cooking Technology Design and Assessment." *Small* 5 (2014): 800.

[14] Anis, Priya, et al. "Customer's Attitude and Satisfaction of Induction (cook-tops) stove in Tirunveli City." IRACST 5.1 (2016): 2319-2828

[15] Agarwal, Paul D., "Eddy-current losses in solid and laminated iron," American Institute of Electrical Engineers, Part I: Communication and Electronics, Transactions of the , vol.78, no.2, pp.169,181, May 1959.

[16] Dodd, C. V., "Some eddy-current problems and their integral solutions,"Oakridge National Laboratories, April 1969.

[17] Llorente, S.; Monterde, F.; Burdio, J.M.; Acero, J., "A comparative study of resonant inverter topologies used in induction cookers,"Applied Power Electronics Conference and Exposition, 2002. APEC 2002.Seventeenth Annual IEEE, vol.2, no., pp.1168, 1174 vol.2, 2002.

[18] Meng, L.C., Cheng, K.W.E. and Chan, K.W., 2009, May. Heating performance improvement and field study of the induction cooker. In *Power Electronics Systems and Applications, 2009. PESA 2009. 3rd International Conference on* (pp. 1-5). IEEE.

[19] Forest, F., Laboure, E., Costa, F. and Gaspard, J.Y., 2000. Principle of a multi-load/single converter system for low power induction heating. *IEEE Transactions on Power Electronics*, *15*(2), pp.223-230.

[20] Semiconductor, O., 2014. Induction Cooking Everything You Need to Know. *Phoenix, Estados Unidos, AND9166/D.*

[21] A. Zahedi, "energy, People, Environment, Development of an integrated renewable energy and energy storage system, an uninterruptible power supply for people and for better environment," The International Conference on Systems, Man, and Cybernetics, 1994.

[22] Viorel B. Modeling solar radiation at the earth's surface: Recent advances. Springer. 2008. ISBN: 3540774548.

[23] S. Pyakuryal and M. Matin "Implementation of AC to DC Converter using Thyristor in ATP," *IOSR Journal of Engineering; vol. 2, Issue 11, pp. 06-11, November 2012.*

[24] J. Doval-Gandoy, C. Castro, and M. C. Martinez "Line Input AC to DC Conversion and Filter Capacitor Design," *IEEE Trans. Industry Application; vol. 39, no.4, pp. 1169-1176,July/August 2003.*

[25] M. H. Rashid, Power Electronics Handbook. Massachusetts: Academic Press, 2007, Chap. 10.

[26] Linden, David, and Thomas B. Reddy. "Handbook of Batteries. 3rd." (2002).

[27] Joseph, Ami, and Mohammad Shahidehpour. "Battery storage systems in electric power systems." *Power Engineering Society General Meeting, 2006. IEEE*. IEEE, 2006.

[28] Distillation, Solar. "Practical Action Technology Challenging Poverty." *Accessed on* 26.07.

[29] S. Llorente, F. Monterde, J. M. Burdio, and J. Acero, "A Comparative Study of Resonant Inverter Topologies Used in Induction Cookers," University of Zaragoza, Zaragoza.

[30] Semiconductor, O., 2014.The Effect of Pan Material in an Induction Cooker. *Denver*, *Colorado*, *AND9201/D*

[31] H. Sarnago, O. Lucia, A. Mediano, and J. M. Burdio, "Dual-Mode-Operation Half-Bridge Resonant Converter for Improved-Efficiency Induction Heating System," Department of Electronic

Appendix A

AC to DC converter calculations

$$V_{dc} == \frac{2.220V}{\pi}\,\frac{2.V_s}{\pi} = 140\ V$$

The DC voltage is 140 volts while the expected is 80 volts DC. The transformer is used to give the ratio in order match the required DC voltage. The ratio is 220 / 80 and that is 2.75. Using the calculated ratio;

$$V_{dc} = \frac{2.80}{\pi} = 50.93\ V$$

The second calculation is the expected load voltage using eq.3;

$$V_L = \frac{V_s}{\sqrt{2}} = \frac{80}{\sqrt{2}} = 56.57\ V$$

The load voltage is 56.57 volts and the 48 volts DC to DC voltage IC is used to regulate the DC value to the required output. The 230V 3 A mains socket is used to power the circuit. The DC and load current are calculated below;

$$I_{dc} = \frac{2.V_s}{\pi.R_L} = \frac{2.80V}{\pi.5ohm} = 10.19\ A$$

$$I_L = \frac{V_s}{\sqrt{2}.R_L} = \frac{80}{\sqrt{2}.5} = 11.31\ A$$

The load resistance is assumed at 5 ohms. The DC and load current are 10.18 A and 11.31 A respectively. Using the above calculations, the expected load power is calculated below;

$$P_L = V_L.I_L = 56.57.11.31 = 639.81\ W$$

And using 48 V DC the power is 542.88 W.

Appendix B

Pot resistance vs. switching frequency

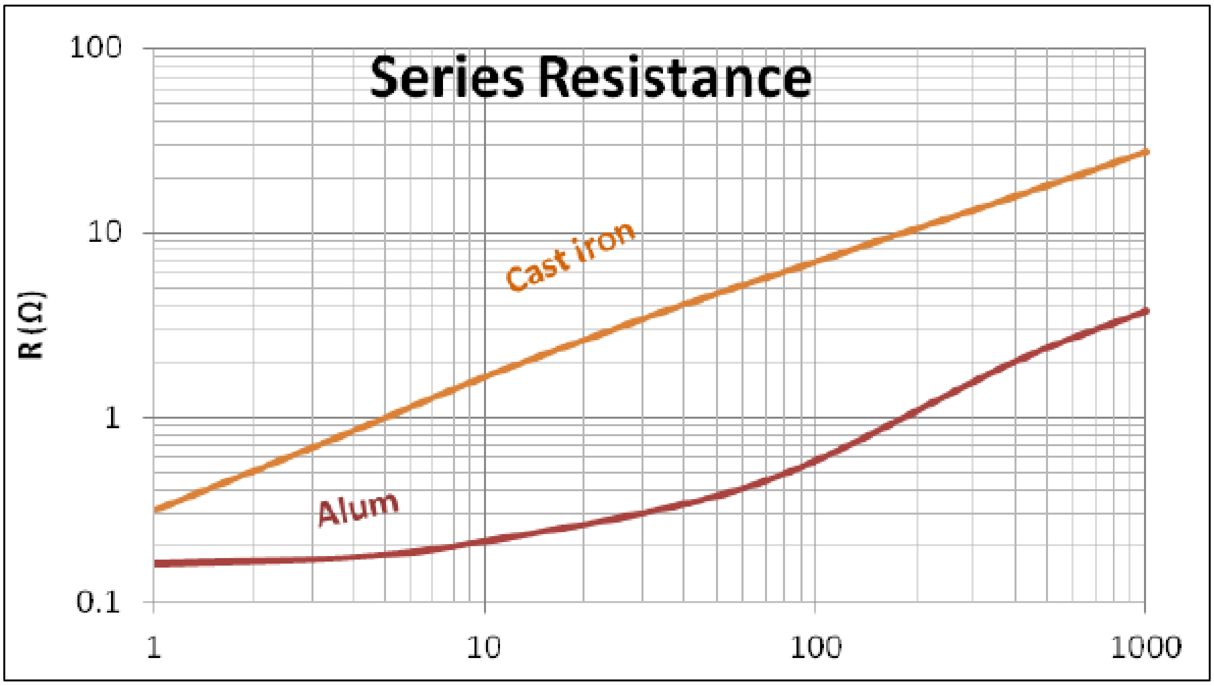

Figure 46: Equivalent series resistance for aluminium and cast iron [30]

Appendix C

Practical and design cost

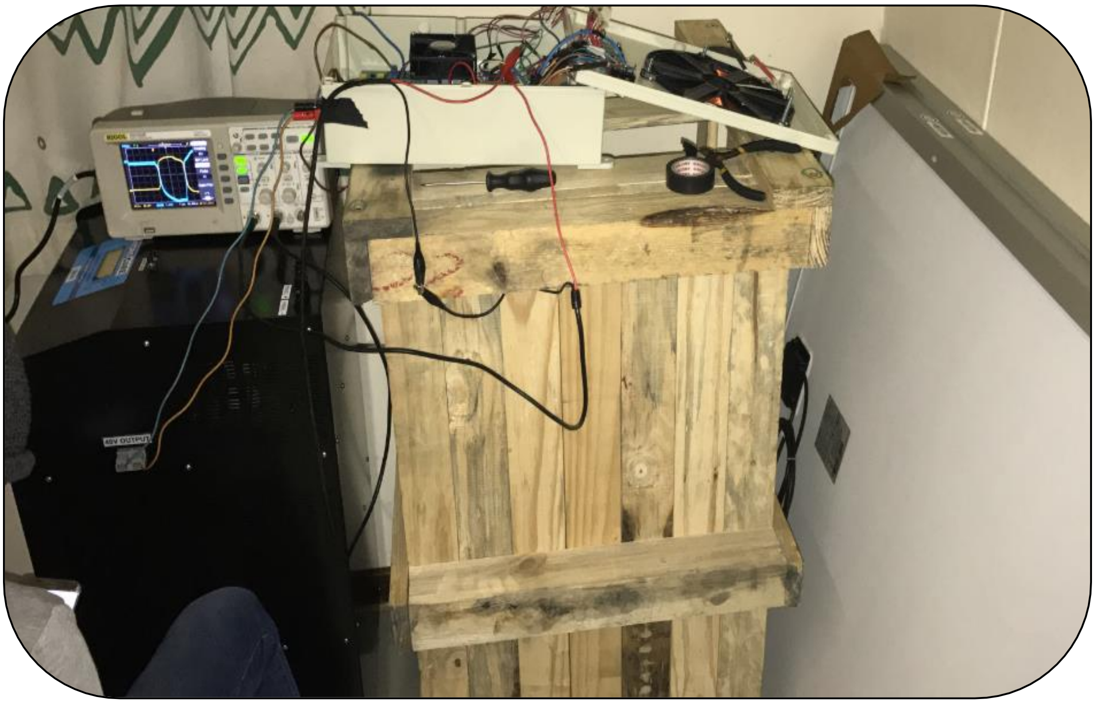

Figure 47: Power unit and deep cycle battery

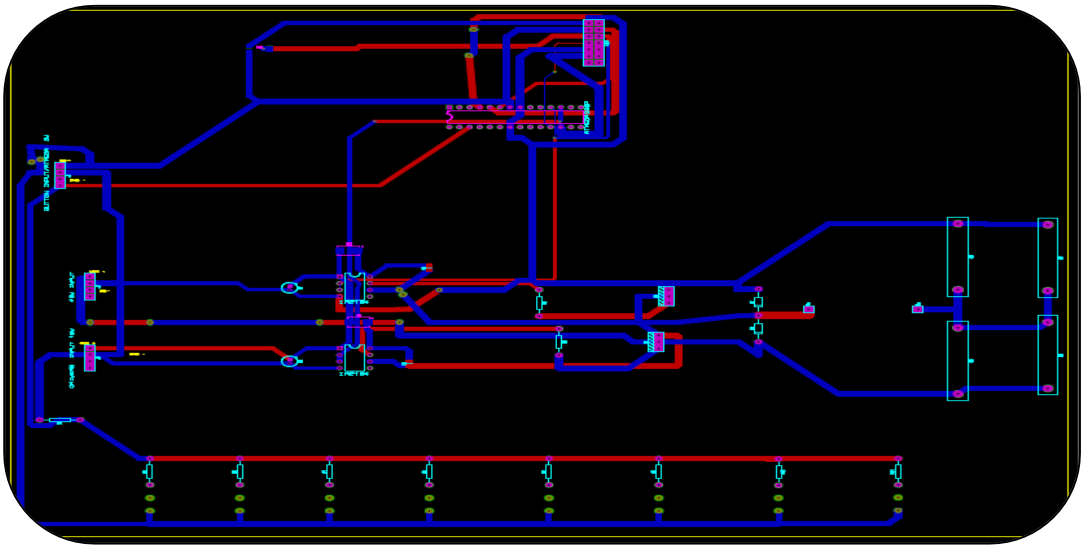

Figure 48: Whole circuit PCB layout

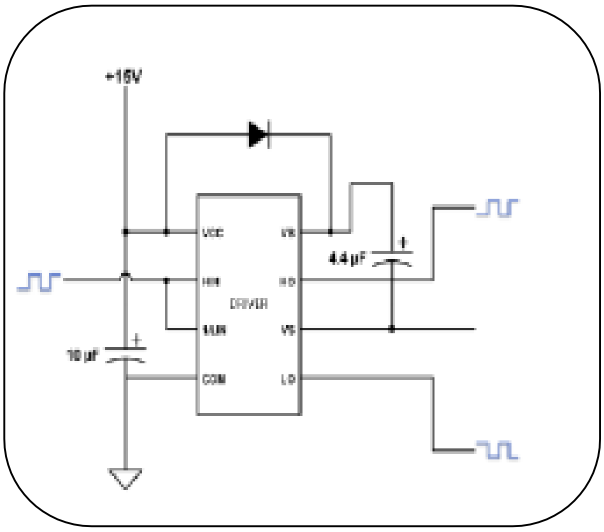

Figure 49: Driver circuit operational diagram

Table C-2: Induction cooker components

Component (s)	Part number	Quantity (s)	Price (Rands)
Capacitors	MKP270	4	10.00
IGBTs	SGL160N60UFD	2	90.00
potentiometer	2k	2	10.00
Decoupling caps	100nF	2	3.00
Atmega	328	1	40.00
LCD	20 x 2	1	80.00
heatsinks	Heatsink	1	20.00
Coil	99.5 uH	1	20.00
			R273.00

Table C-2: other components for complete solar system unit

Component (s)	Part number	Quantity (s)	Price (Rands)
Batteries	Dixon DC 105ST 12V	4	20 700.00
Whole PSU comp	500 W 48V DC	1	11 900.00
Solar panels	SOL310-RNW	2	9 500.00
			R 42 100.00

Table C-3: Electric stove (2 plates) consumption

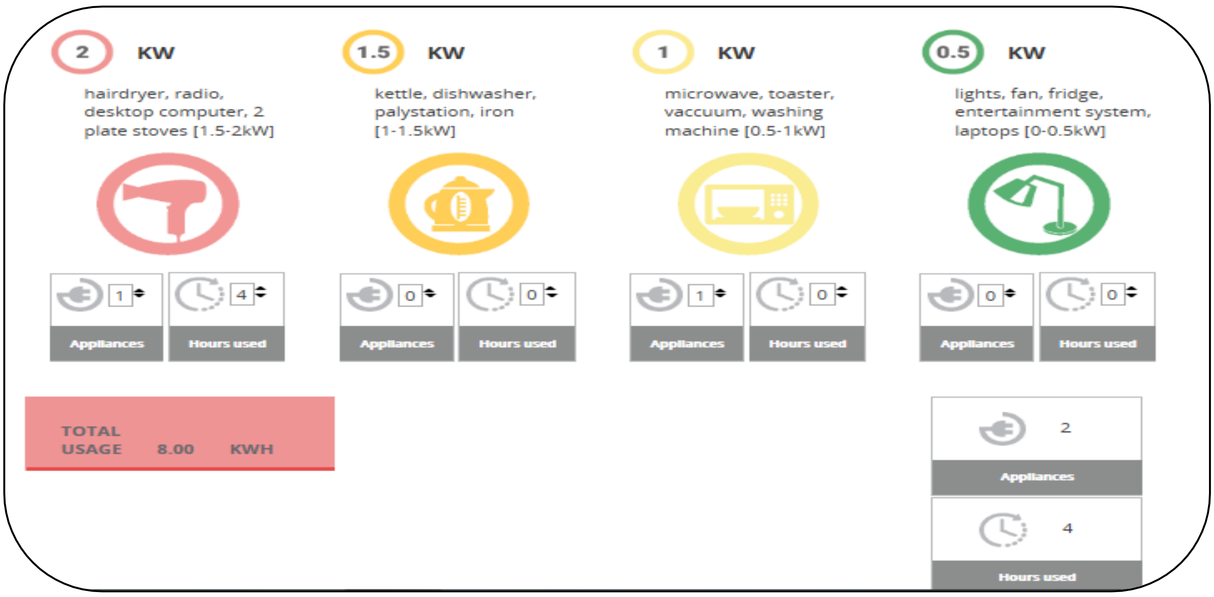

Appendix D

Code for the whole circuit operation

```
#include <LiquidCrystal.h>

#include <PWM.h>

#include <Wire.h>

// initialize the library with the numbers of the interface pins

LiquidCrystal lcd(12, 11, 7, 4, 3, 2);

float voltage = 0.0;

int powerSource = 0;

int led = 13;

int Q1 = 5;

int Q2 = 6;

int powerlevel = 0;

void setup()

{

 pinMode(Q1, OUTPUT);

  pinMode(Q2, OUTPUT);

//DDRD = DDRD | B11111100;  // set PORTD (digital 7~0) to outputs

 lcd.begin(20,2);// set up the LCD's number of columns and rows:

Serial.begin(9600);

pinMode(led, OUTPUT);

}

void loop() {

// the loop routine runs over and over again forever:


  // read the input on analog pin 0:
```

```
  float sensorValue = analogRead(A3);

  // Convert the analog reading (which goes from 0 - 1023) to a voltage (0 - 5V):

  float voltage = sensorValue * (4.97 / 1023.00);

if( voltage > 0.5 && voltage <= 1.24){

powerlevel = 1;

}

else if (voltage > 1.44 && voltage <= 1.74){

  powerlevel = 2;

}

 else if (voltage > 1.84 && voltage <= 2.14){

  powerlevel = 3;

}

else if ( voltage > 2.24 && voltage <= 2.74){

  powerlevel = 4;

}

else if (voltage > 2.84 && voltage <= 3.14){

  powerlevel = 5;

}

else if (voltage > 3.24 && voltage <= 3.74){

  powerlevel = 6;

}

else if (voltage > 3.84 && voltage <= 4.34){

  powerlevel = 7;

}

else if (voltage > 4.44 && voltage <= 4.96){

  powerlevel = 8;

}
```

```
switch(powerlevel){
      case 1:
         lcd.clear();
         // Print a message to the LCD.
         lcd.setCursor(0, 0);
         lcd.print("SW Frequenc, 62.5kHz");
         lcd.setCursor(0, 1);
         lcd.print("Power, 300W");
          digitalWrite(led, HIGH);

  digitalWrite(Q2, HIGH);
//PORTD = B01000000; //pin 6 is high
delayMicroseconds(6);
digitalWrite(Q2, LOW);
//digitalWrite(Q1, LOW);
//PORTD = B00000000; //all pins are off 0.00
delayMicroseconds(1);
digitalWrite(Q1, HIGH);
//PORTD = B00100000; //pin 5 is high
delayMicroseconds(6);
//digitalWrite(Q2, LOW);
digitalWrite(Q1, LOW);
//PORTD = B00000000;//all pins are off
delayMicroseconds(1);
       break;
       case 2:
          lcd.clear();
```

```
        // Print a message to the LCD.
        lcd.setCursor(0, 0);
        lcd.print("SW Frequenc, 50kHz");
        lcd.setCursor(0, 1);
        lcd.print("Power, 450W");
         digitalWrite(Q2, HIGH);
//PORTD = B01000000; //pin 6 is high
delayMicroseconds(8);
digitalWrite(Q2, LOW);
//digitalWrite(Q1, LOW);
//PORTD = B00000000; //all pins are off
delayMicroseconds(1);
digitalWrite(Q1, HIGH);
//PORTD = B00100000; //pin 5 is high
delayMicroseconds(8);
//digitalWrite(Q2, LOW);
digitalWrite(Q1, LOW);
//PORTD = B00000000;//all pins are off
delayMicroseconds(1);


      break;
      case 3:
        lcd.clear();
        // Print a message to the LCD.
        lcd.setCursor(0, 0);
        lcd.print("SW Frequenc, 41.67kHz");
        lcd.setCursor(0, 1);
```

```
        lcd.print("Power, 720W");
         digitalWrite(Q2, HIGH);
//PORTD = B01000000; //pin 6 is high
delayMicroseconds(10);
digitalWrite(Q2, LOW);
//digitalWrite(Q1, LOW);
//PORTD = B00000000; //all pins are off
delayMicroseconds(2);
digitalWrite(Q1, HIGH);
//PORTD = B00100000; //pin 5 is high
delayMicroseconds(10);
//digitalWrite(Q2, LOW);
digitalWrite(Q1, LOW);
//PORTD = B00000000;//all pins are off
delayMicroseconds(2);
      break;
      case 4:
        lcd.clear();
        // Print a message to the LCD.
        lcd.setCursor(0, 0);
        lcd.print("SW Frequenc, 35.71kHz");
        lcd.setCursor(0, 1);
        lcd.print("Power, 780W");
        digitalWrite(Q2, HIGH);
//PORTD = B01000000; //pin 6 is high
delayMicroseconds(12);
digitalWrite(Q2, LOW);
```

```
//digitalWrite(Q1, LOW);
//PORTD = B00000000; //all pins are off
delayMicroseconds(3);
digitalWrite(Q1, HIGH);
//PORTD = B00100000; //pin 5 is high
delayMicroseconds(12);
//digitalWrite(Q2, LOW);
digitalWrite(Q1, LOW);
//PORTD = B00000000;//all pins are off
delayMicroseconds(3);
    break;
    case 5:
      lcd.clear();
      // Print a message to the LCD.
      lcd.setCursor(0, 0);
      lcd.print("SW Frequenc, 27.78kHz");
      lcd.setCursor(0, 1);
      lcd.print("Power, 900W");
      digitalWrite(Q2, HIGH);
//PORTD = B01000000; //pin 6 is high
delayMicroseconds(14);
digitalWrite(Q2, LOW);
//digitalWrite(Q1, LOW);
//PORTD = B00000000; //all pins are off
delayMicroseconds(4);
digitalWrite(Q1, HIGH);
//PORTD = B00100000; //pin 5 is high
```

```
delayMicroseconds(14);
//digitalWrite(Q2, LOW);
digitalWrite(Q1, LOW);
//PORTD = B00000000;//all pins are off
delayMicroseconds(4);
    break;
    case 6:
      lcd.clear();
      // Print a message to the LCD.
      lcd.setCursor(0, 0);
      lcd.print("SW Frequenc, 20kHz");
      lcd.setCursor(0, 1);
      lcd.print("Power, 780W");
       digitalWrite(Q2, HIGH);
//PORTD = B01000000; //pin 6 is high
delayMicroseconds(19);
digitalWrite(Q2, LOW);
//digitalWrite(Q1, LOW);
//PORTD = B00000000; //all pins are off
delayMicroseconds(4);
digitalWrite(Q1, HIGH);
//PORTD = B00100000; //pin 5 is high
delayMicroseconds(19);
//digitalWrite(Q2, LOW);
digitalWrite(Q1, LOW);
//PORTD = B00000000;//all pins are off
delayMicroseconds(4);
```

```
      break;
      case 7:
        lcd.clear();
        // Print a message to the LCD.
        lcd.setCursor(0, 0);
        lcd.print("SW Frequenc, 15.15kHz");
        lcd.setCursor(0, 1);
        lcd.print("Power, 840W");
        digitalWrite(Q2, HIGH);
//PORTD = B01000000; //pin 6 is high
delayMicroseconds(21);
digitalWrite(Q2, LOW);
//digitalWrite(Q1, LOW);
//PORTD = B00000000; //all pins are off
delayMicroseconds(4);
digitalWrite(Q1, HIGH);
//PORTD = B00100000; //pin 5 is high
delayMicroseconds(21);
//digitalWrite(Q2, LOW);
digitalWrite(Q1, LOW);
//PORTD = B00000000;//all pins are off
delayMicroseconds(4);
      break;
      case 8:
        lcd.clear();
        // Print a message to the LCD.
        lcd.setCursor(0, 0);
```

```
        lcd.print("SW Frequenc, 10kHz");
        lcd.setCursor(0, 1);
        lcd.print("Power, 2160W");
         digitalWrite(Q2, HIGH);
//PORTD = B01000000; //pin 6 is high
delayMicroseconds(24);
digitalWrite(Q2, LOW);
//digitalWrite(Q1, LOW);
//PORTD = B00000000; //all pins are off
delayMicroseconds(4);
digitalWrite(Q1, HIGH);
//PORTD = B00100000; //pin 5 is high
delayMicroseconds(24);
//digitalWrite(Q2, LOW);
digitalWrite(Q1, LOW);
//PORTD = B00000000;//all pins are off
delayMicroseconds(4);
      break;
      default:
         lcd.clear();
         // Print a message to the LCD.
         lcd.setCursor(0, 0);
         lcd.print("SELECT POWER LEVEL");

}

}
```